AUT Journal of Civil Engineering

AUT J. Civil Eng., 4(4) (2020) 449-472
DOI: 10.22060/ajce.2020.16390.5584

Investigating the Effect of Particle Size on the Anisotropic Behavior of Saturated Sands, Using Hollow Cylindrical Torsional Shear Apparatus

A. Mohammadi, H. Bahadori*

Civil Engineering Department, Urmia University, Urmia, Iran.

ABSTRACT: The inherent anisotropic behavior of sands and the grain size effects are studied in this paper. A series of undrained torsional shear tests with constant inclination angle (α°) and intermediate principal stress ratio (b) was conducted by hollow cylindrical torsional apparatus (HCTA) on four types of sand. This study furthers the knowledge on the dependency of steady states on anisotropy sands with different shape and size properties. In doing so, the direction of principal stress orientation is varied from 15° to 60°, for an intermediate principal stress ratio of 0.5 and 1.0 and constant initial confining pressure. The results show that by increasing the particle sizes, the behavior of sands changes from contractive behavior to fully hardening and dilative behavior. Also, it observed that the effect of anisotropy in coarse grain sands is more than fine grain sands. In this study two-dimensional image analysis has been adapted to classify particle shape properties. These morphological characteristics were determined from the analysis of scanning electron microscope images and were defined as sphericity and roundness. The results of the experiments on all four types of sand show that the anisotropy effects decrease by increasing the sphericity, but in coarse grain sands, the roundness of grains has no much effect on the behavior and anisotropy.

Review History:
Received: May, 20, 2019
Revised: Nov. 09, 2019
Accepted: May. 13, 2020
Available Online: May. 27, 2020

Keywords:
Hollow Cylindrical Torsional - Apparatus (HCTA)
Inherent Anisotropy
Sand, Grain Sizes
Undrained Shear Strength.

1- Introduction

Study on compressibility characteristics and shear behavior of soils according to the anisotropy phenomenon are extremely important for the accurate design of foundations and stability analysis of earth structures. Designing the foundations of offshore structures, deep excavations, embankments, and dikes, and other earth structures needs to necessitate critical situations, such as directions and values of the principal stresses. The directional dependency of the physical and mechanical behavior of soils is known as the anisotropy phenomenon. The process of sedimentation in soil formation arranges the particles in a preferred direction, which is known as the soil stratification or bedding direction. Load direction changes relative to stratification orientation change the behavior of soil, which is known as the inherent anisotropy effect [1]. The grain size distribution of a soil determines the governing particle-level forces, inter-particle packing, and the ensuing macro-scale behavior; therefore, grain size distribution plays a central role in soil classification systems. Various researches are conducted on the anisotropic behavior of sandy soils during recent years. Studies conducted on these soils express that the size of particles affects significantly the behavior and shear strength of sandy soils. However, the anisotropy of sand has not been fully studied in terms of the effects of different grain shapes and sizes. To conduct a comprehensive study on the anisotropic strength properties of soil materials, it is required to have a device to monitor and control not only the three principal stresses but also the major principal stress. This device should also be able to control the drainage and pore water pressure. The hollow cylindrical torsional shear apparatus (HCTA) employed by Ishihara and Towhata [2] and Pradel et al. [3] was improved with automatic stress and strain control system using a personal computer. The method of calculation of stresses and strains was described by Pradhan et al. [4] and Pradel et al. [3]. Many tests by HCTA have been conducted to prove the anisotropy effect on sandy soils [5-8]. the strength and deformation characteristics of Most natural sands are anisotropic [9]. Yoshimine et al. [8] studied the effect of inherent anisotropy (i.e., different behavior in different loading directions) in Toyoura sand. He observed that when the inclination of the major principal stress concerning the depositional (vertical) direction (α) becomes larger, the behavior of sand softens and be more contractive. As reported by Yoshimine et al. [8] in α=15°, the pore water pressure ratio excessed only 20% and the behavior of sand was hardening, On the other hand, when α=75°, pore water pressure ratio developed up to nearly 90% and the behavior was a strain-softening behavior. Uthayacumar and Vaid [7] and Sivathayalan and Vaid [5] reported the same results. The considerable dependence of the sand behavior to the inclination angle indicates the inherent anisotropy in the material due to the soil particle

*Corresponding author's email: h.bahadori@urmia.ac.ir

arrangement. In addition to the inclination, the intermediate stress ratio is the other index of inherent anisotropy. Parameter $b = (\sigma_2 - \sigma_3)/(\sigma_1 - \sigma_3)$ defines this effect very well. When the intermediate principal stress increases, the sand tends to have softer behavior. Yang et al. [10] studied the influence of *b* parameter on the deformation characteristics and pore pressure response of Toyoura sands during cyclic rotation of principal stress axes. The investigation was conducted in an automated hollow cylinder. A total of 12 cyclic undrained shear tests were conducted with b = 0, b= 0.5 and b= 1.0. They observed that the rate of pore pressure generation in b=0 was much slower than that under the conditions b = 0.5 and b=1.0. This observation shows that in lower b value the soil resistance to pore pressure build-up is much stronger. In another research, Shahnazari and Towhata [11] observed that when a soil sample is subjected to cycling loading, its density increases due to the shear deformations. This change affects the stress–strain behavior of soil in the following stages of shearing. During cyclic shear, besides the effects of density, shear history affects the behavior of sands.

Bahadori et al. [12] studied the effect of inherent anisotropy on the undrained behavior of sands using hollow cylindrical torsional apparatus (HCTA). They observed that when the intermediate stress parameter (b) is constant, increasing the inclination angle concerning the depositional direction (α) decreases the strength in pure sand. At α=75°, limited flow or quasi-steady-state behavior is attained. At lower α values, the strain-softening behavior did not occur, and the dilatant behavior was dominant. In all of the pure sand tests, the phase transformation exhibits the conventional behavior in cases of medium-dense sand. The same results have been reported by khayat et al. [13].

In the last few decades, numerous laboratory tests have been performed to evaluate the influence of particle size as well as numerical tests. The variety of the conclusions revealed an ambiguity which leads to further investigations. Holtz and Gibbs [14]conducted a series of triaxial tests on mixtures of sand and gravel and concluded that by increasing the gravel content greater than 50–60 % (by weight) the shear strength increases. Frederick [15] indicated that the behavior of granular materials changed with the alteration of particle size. Kolbuszewski and Frederick [16] reported that the macroscopic response of the granular soil is the summation of the deformation of the mass before crushing depends on the individual soil grain size and the individual response of the particles. To investigate the influence of particle size, Kolbuszewski and Frederick used glass beads and concluded that by increasing the grains size the maximum porosity decreases, and compressibility increases. Zolkov and Wiseman [17] conducted tri-axial tests on sands and observed that an increase in grain size, increases the angle of shearing resistance. Kolbuszewski and Frederick reported similar conclusions to Zolkov and Wiseman but Kirkpatric [18] found different results. According to Kirpatric, the angle of shearing resistance decreases with the increase of grain size, which agreed with the findings reported in Marschi et al. [19]. To determine the effect of particle size Chattopadhya [20] performed a series of direct shear tests using Mogra sand and described that the fabric of the granular mass is a function of the grain sizes and their distribution and the maximum void ratio increase with the decrease of particle size while Kirpatric reported maximum and minimum void ratios remain constant with the particle size. From the numerical observations, Sitharam [21] described that due to change of the particle size and gradation, shear behavior of granular mass changes. A change of particle gradation maintaining the minimum particle size as constant, results in the decrease in the angle of internal friction and also increase in volumetric strain. Islam et al. [22] conducted the direct shear tests on sand samples with granules of uniform particles in small medium and large size and concluded that the shear strength of the samples is increased by increasing the grain size. Vangla and Gali [23] concluded by conducting the direct shear tests on three types of sand with different sizes, that the peak strength of sands is not different significantly according to the stress-strain diagrams, but the ultimate strength of the sand with larger particle size is larger than the small size sands. In addition, the changes in the volume of the sand samples with larger particle size indicated more dilative behavior compared to the other samples.

In this study, four types of poorly graded sand with different sizes were used. Hollow cylindrical torsional shear tests were conducted on three maximum angles of principal stresses with the vertical axis of 15, 30, and 60 degrees to examine the effect of grain size on the un-drained behavior of saturated sands, and two intermediate principal stress ratio of 0.5 and 1 were used. It should be noted that little research has been conducted on the effect of the size of the sand particles on the anisotropic behavior of saturated sand. It can be stated that the results of this study will be able to eliminate the ambiguity about the effect of physical characteristics on the anisotropic behavior of the sands according to the above-mentioned cases.

2- Materials and Methods

2.1. Material properties

In this study, four types of poorly graded sand with different sizes were used. These sands contain two types of silicate Firoozkuh sands No. 131 and No.161, quartz sand of Urmia Lake, and quartz sand of Leighton buzzard. The sands of Firoozkuh and the Leighton buzzard are both industrial and Urmia Lake sand is made of the shores of Urmia Lake and is a natural type. Figure 1 shows the grading diagram of these four types of sand. This study uses Urmia Lake (UL) and Firoozkuh No. 161 (F161) sands as fine graded sands and Leighton Buzzard (LB) and Firoozkuh No. 131 (F131) sand grains are used as coarse graded sand. Figure 2 shows the images taken of materials applied in this study by the electrical microscope.

According to Krumbein and Sloss [24], Cho et al [25], the distinguishing features in the shapes of the particles are based on their sphericity and also their roundness. The definition of these two important scales is given below:

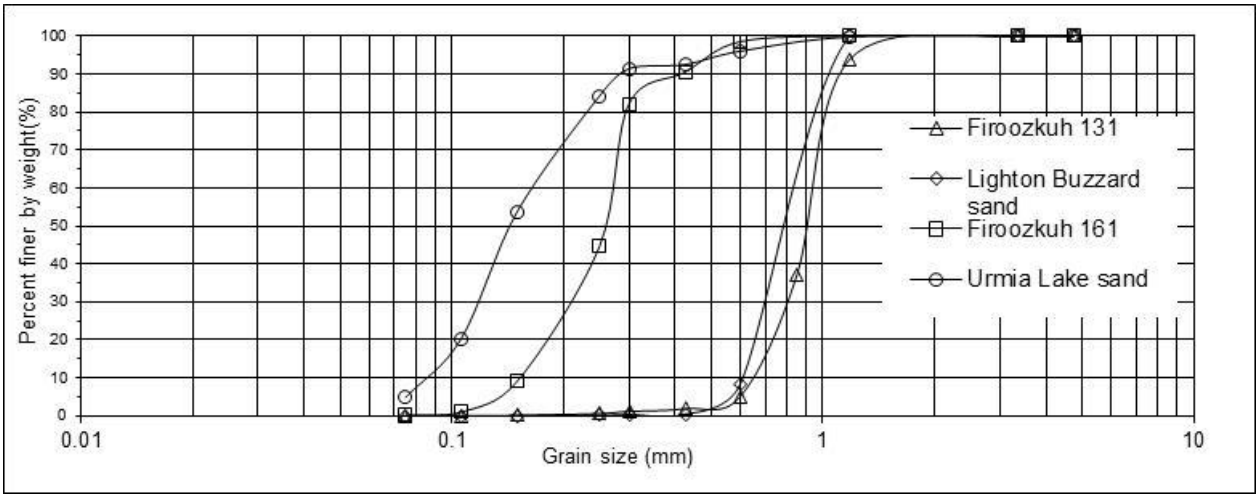

Fig. 1. Grain size distribution curves of four grains of sand.

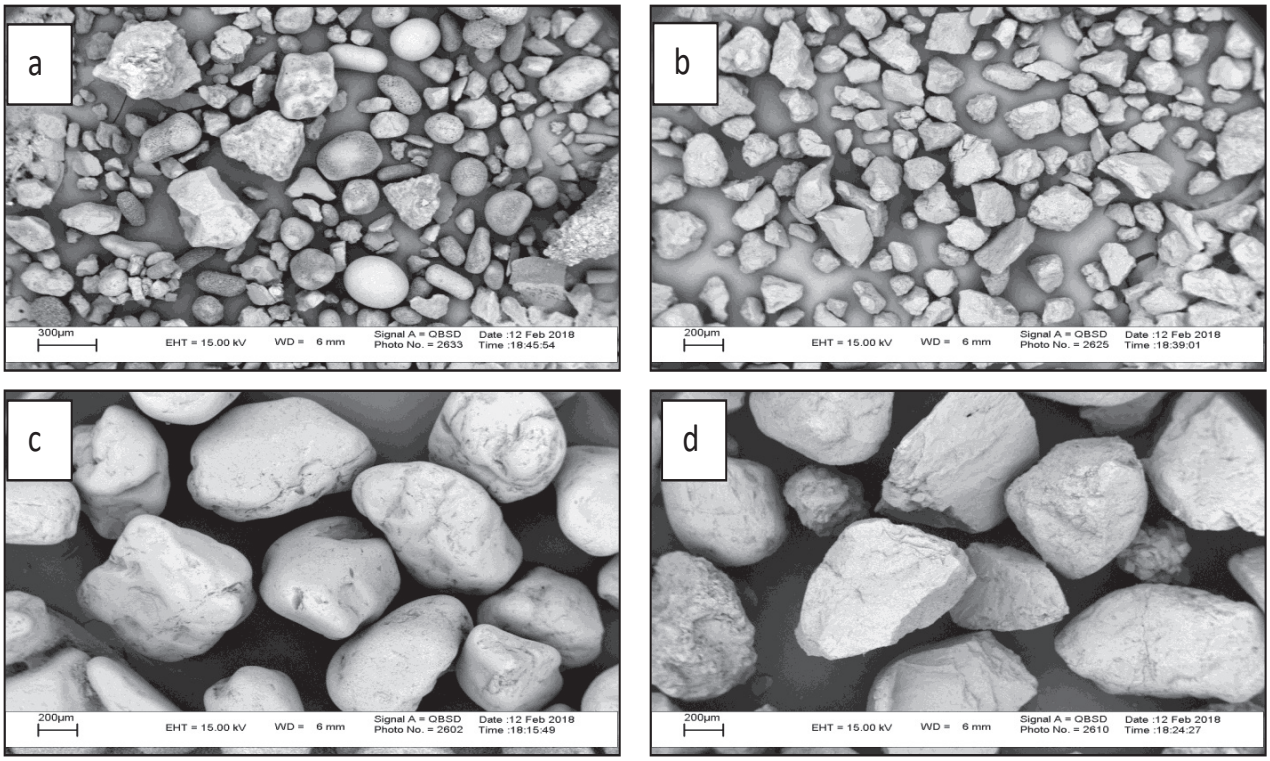

Fig. 2. Scanning electron microscopic (SEM) images (a) Urmia lake sand (b) Firoozkuh No. 161 sand (c) Leighton buzzard sand (d) Firoozkuh No. 131 sand.

- Sphericity (S), ($S = \frac{r_{max-in}}{r_{min-cir.}}$) determined by obtaining the radius of the largest inscribed sphere (r_{max-in}) relative to the radius of the smallest circumscribed sphere ($r_{min-cir}$).
- Roundness (R), ($R = \frac{\sum r_i / N}{r_{max-in}}$) is quantified as theaverage radius of curvature of features relative to the radius of the maximum sphere that can be inscribed in the particle. The relationship between the sphericity and roundness can be further defined and evaluated in the form of dimensionless parameters as shown in Fig.3 [24, 25].

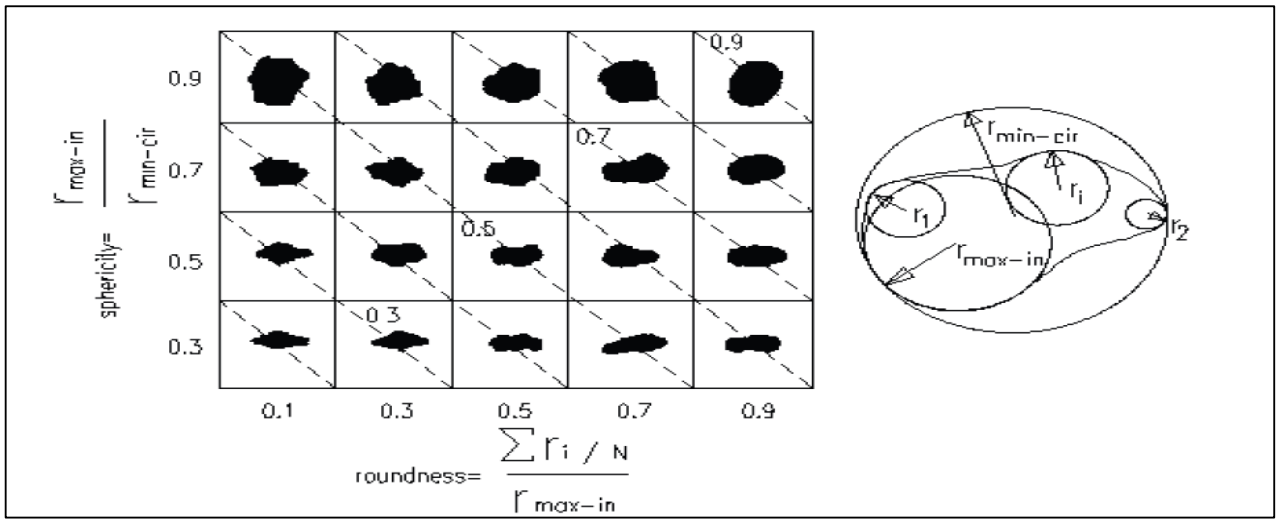

Fig. 3. Particle shape definition (Krumbein and Sloss [24], Cho et al [25]).

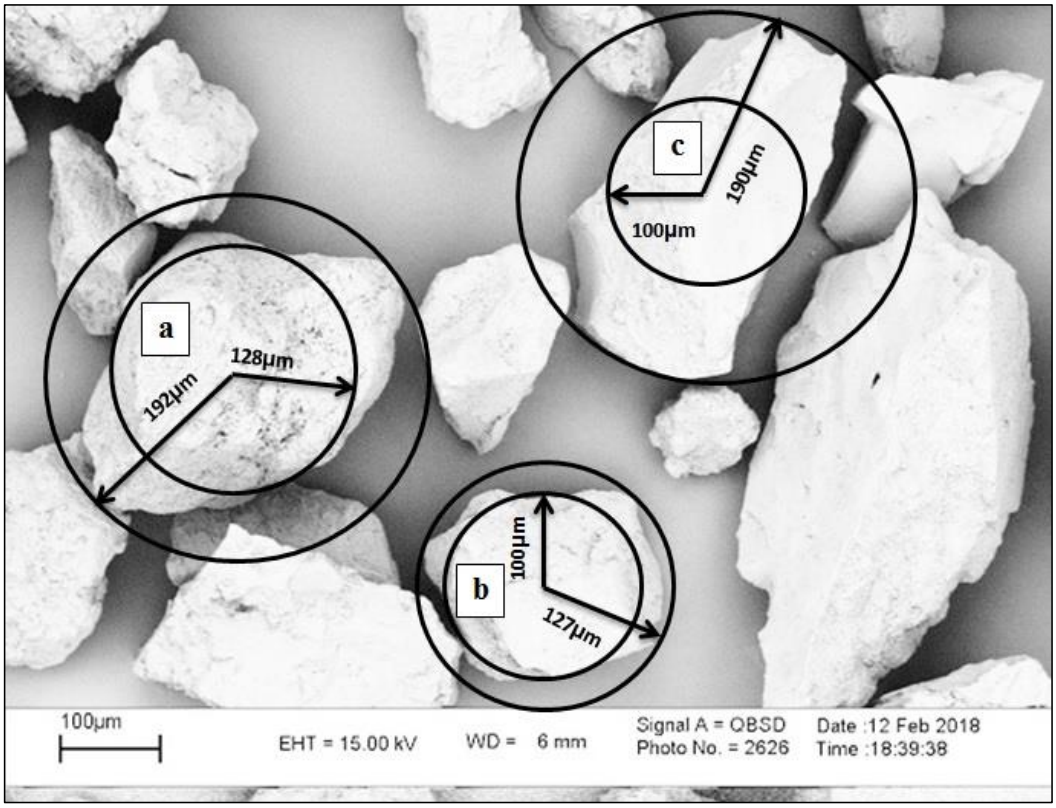

Fig. 4. Measurement of the sphericity of grains for sand F161

a) r_{max-in} =128µm, $\sum r_i / N = 46.67\mu m$, $S_a = 0.666$

b) r_{max-in} =100µm, $\sum r_i / N = 127\mu m$, $S_b = 0.787$

c) r_{max-in} =100µm $\sum r_i / N = 190\mu m$, , $S_c = 0.526$

Table 1. Physical characteristics of sands

Sand	D_{10}	D_{50}	D_{60}	C_u	C_c	Sphericity	Roundness	e_{min}	e_{max}
Urmia lake	0.08	0.15	0.17	1.16	2	0.65	0.69	0.523	0.801
Firuzkooh 161	0.16	0.72	0.28	0.96	1.78	0.683	0.3	0.548	0.874
Leighton Buzzard	0.61	0.82	0.89	0.9	1.45	0.68	0.73	0.574	0.725
Firuzkooh 131	0.65	0.91	0.94	1.04	1.44	0.695	0.43	0.640	0.940

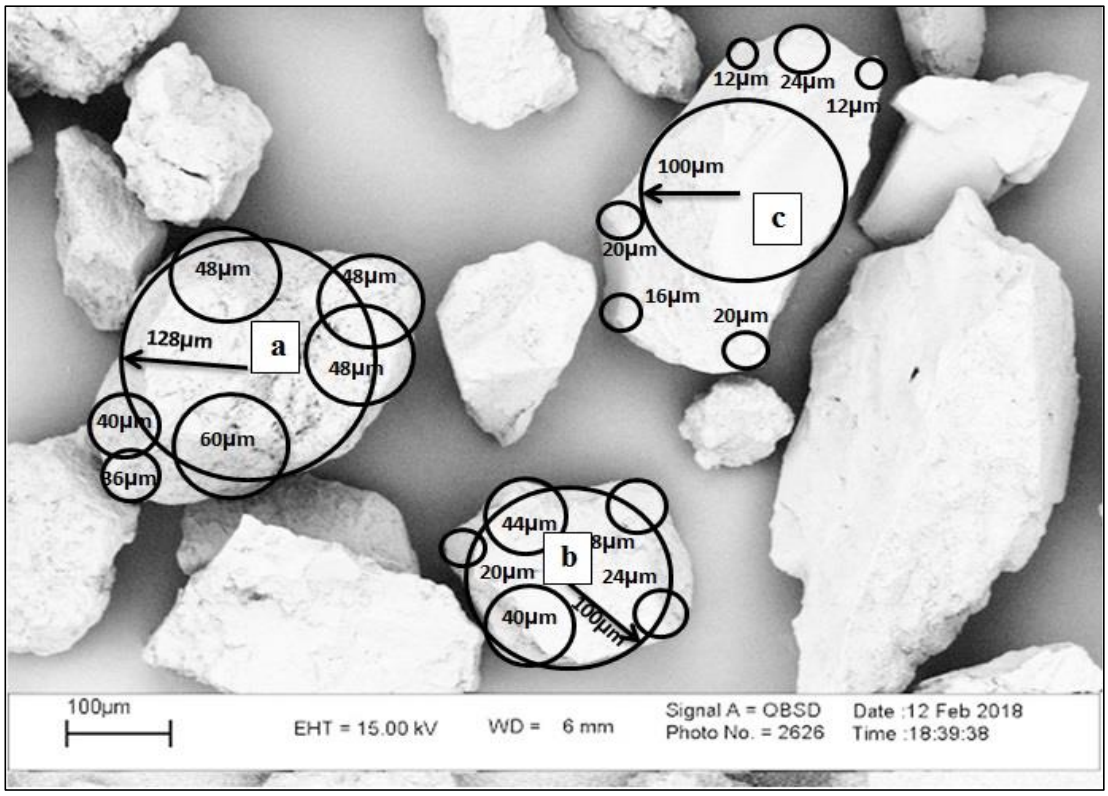

Fig .5. Measurement of the roundness of grains for sand F161

a) r_{max-in} =128µm, $\sum r_i / N = 46.67\mu m$, $R_a = 0.364$

b) r_{max-in} =100µm, $\sum r_i / N = 31.2\mu m$, $R_b = 0.312$

c) r_{max-in} =100µm, $\sum r_i / N = 31.2\mu m$, $R_c = 0.173$

In this study, 2D image analysis is used to calculate grain shape parameters. In this method, 50 soil grains were randomly photographed using electrical microscopes, and sphericity and roundness parameters are then calculated separately for each of the grains using the method presented by Krumbein and Sloss[24]and Cho et al[25]). At last, averaging them for each of the grains, the sphericity, and roundness of sands is calculated as the dimensionless parameters of shape. Fig. 4 and 5 show the way calculate of calculating the sphericity and roundness of grains for sand F161. Table 1 shows the values of sphericity and roundness parameters and the physical features of the materials used in this study.

2.2. Methods - HCTA Specimens Synthesis

Several methods exist for remoulding granular soils sample at a laboratory-scale. The base soil can be moist, dry, or saturated; it can be placed through dry deposition, water sedimentation, pouring, or spooning; and maybe compacted by tapping, tamping, or vibration. In this study, the dry deposition method was used as a sample preparation technique. The dry deposition method prepares more uniform sandy specimens [12, 13]. Before the saturation stage, Carbon dioxide (CO_2) and de-aired water were passed through the specimen. After the preparation of the sample, the saturation stage continued till achieved a Skempton value of B≥0.96.

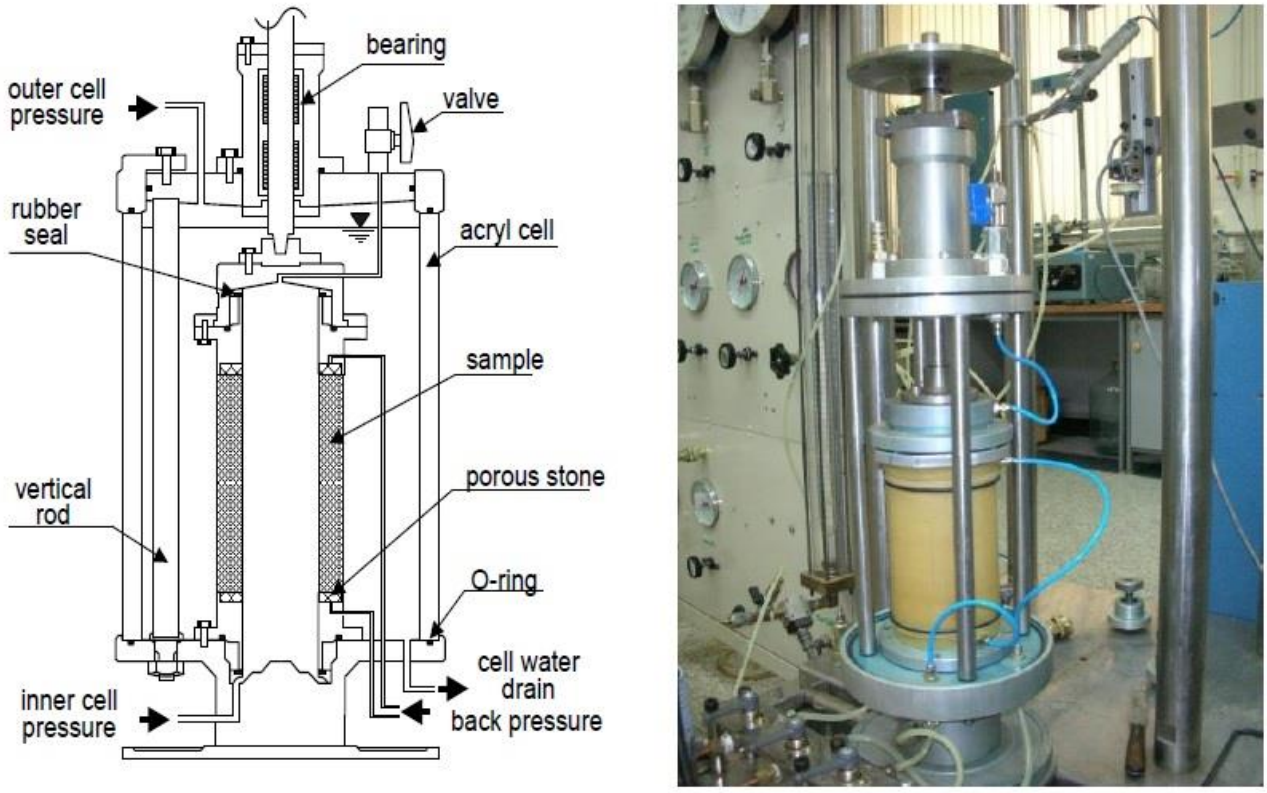

Fig. 6. Schematic diagram of hollow cylinder torsional apparatus (HCTA) and a specimen in the test using HCTA.

The samples isotropically consolidated to avoid the induced anisotropy effect (P′c=200 kPa). All the tests conducted were consolidated undrained (CU). The shear stage started after the consolidation stage, where the rate of torque-speed was 0.5 degrees/min, the lowest speed that can be applied to the system. The porosity of the samples was measured, at the end of the tests.

2.3. Methods – Apparatus

Soil behavior is fundamentally stressed path-dependent. The stress path for geotechnical structures involves rotating principal stress directions about three axes. The conventional triaxial shear apparatus falls short in not offering control over the principal stress directions. The Hollow Cylinder Torsional Shear (HCTS) apparatus allows simultaneous application of axial load, torque, internal and external pressures; and hence incorporates a control on both principal stress direction and intermediate principal stress into the stress path approach. HCTS offers an opportunity for a better understanding of soil's inherent anisotropy and its implications on stress-strain [post-peak] behavior. Fig.6 illustrates the HCTS apparatus together with a specimen in the test

A series of consolidated undrained (CU) tests were conducted on reinforced sand specimens. To apply the inner and outer cell pressure, in addition to the axial and torsional loads pneumatic actuators, 4 electrical/pneumatic (*E/P*) transducers were utilized. In total, 11 transducers were used. To capture the post-peak soil behavior, a step motor for torsional strain tests was used. The speed of the cylinder twist in all tests was retained at low 0.5°.min^{-1}, the lowest possible torque rate offered by the apparatus. The principal stress direction (α°) and intermediate principal stress ratio (b) were retained constant throughout the torsional shear tests.

The inner chamber is isolated from the outer confining chamber, allowing the variation of stress at the inner boundary of the test specimen to be completely independent of that of the outer boundary. Whilst the apparatus allows the adoption of similar inner and outer cell pressures, in the present work, the inner cell pressure (P_i) and outer confining pressure (P_0) applied were not equal.

Symes [6] proposed Eqs. (1) to (5) formulate the circumferential normal stress σ_θ, vertical normal stress σ_z, radial normal stress σ_r and shear stress $\sigma_{z\theta}$ that apply to the wall of the specimen. Confining pressures are formulated as a function of circumferential and radial stresses in Eq. (5).

$$\sigma_\theta = \sigma_z - \frac{2\tau_{z\theta}}{tan\,2\alpha} \tag{1}$$

$$\sigma_r = \sigma_z - \frac{\sigma_{z\theta}\left(Cos\,2\alpha - 2b + 1\right)}{sin\,2\alpha} \tag{2}$$

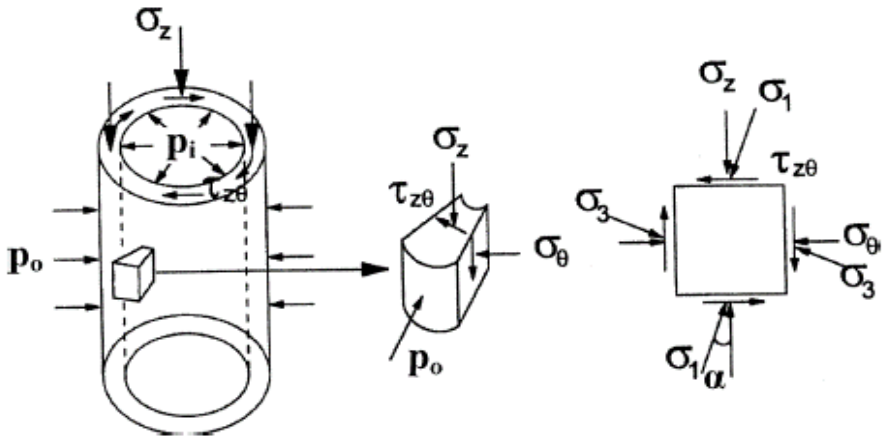

Fig. 7. Stress state in the wall of hollow cylinder specimen during torsion shear test (Lade and Rodriguez [26])

$$\tau_{z\theta} = \frac{1}{2}\left\{\frac{3T}{2\pi\left(r_0^3 - r_i^3\right)} + \frac{T}{\pi\left(r_0^2 + r_i^2\right)\left(r_0 - r_i\right)}\right\} \quad (3)$$

$$\sigma_z = \frac{F_v + \pi\left(p_0 r_0^2 - p_i r_i^2\right) - A_r p_0}{A_s} \quad (4)$$

$$\begin{cases} P_i = \dfrac{\sigma_r\left(r_0 + r_i\right) - \sigma_\theta\left(r_0 - r_i\right)}{2r_i} \\ P_0 = \dfrac{\sigma_r\left(r_0 + r_i\right) - \sigma_\theta\left(r_0 - r_i\right)}{2r_\theta} \end{cases} \quad (5)$$

Where r_i and r_o are current inner and current outer radius of the sample and T is monotonic torque. F_v is the surface tractions-vertical force. A_r and A_s are cross-section areas for axial road and the sample, respectively. HCTS load and stress conditions are graphically illustrated in Fig.7.

The principal stresses are formulated in Eqs. (6) to (8). σ_1 is the major principal stress, σ_2 is intermediate principal stress, and σ_3 is minor principal stress respectively.

$$\sigma_1 = \frac{\sigma_z + \sigma_\theta}{2} + \sqrt{\left(\frac{\sigma_z - \sigma_\theta}{2}\right)^2 + \tau_{z\theta}^2} \quad (6)$$

$$\sigma_2 = \sigma_r \quad (7)$$

$$\sigma_3 = \frac{\sigma_z + \sigma_\theta}{2} - \sqrt{\left(\frac{\sigma_z - \sigma_\theta}{2}\right)^2 + \tau_{z\theta}^2} \quad (8)$$

3- Results and Discussion

The results of undrained hollow cylindrical torsional shear tests are used to examine the effect of grain shape and size on the anisotropic behavior of saturated sands. These experiments are conducted with a primary consolidating pressure of 200 kPa, in three inclination angles of the major principal stress of 15, 30, and 60 degrees, and two intermediate principal stress ratios of 0.5 and 1. Table 2 shows the specifications of the conducted tests. Inclination angle concerning the depositional (vertical) direction (α°), intermediate stress ratio (b), void ratio after consolidation (e), and relative density (D_r) were the variables in the tests (Table 2).

3.1. Anisotropy and steady states

Important research developments achieved in the study of the mechanical behavior of saturated sands under undrained conditions are regularly related to the problem of stability of sand masses subjected to quick loadings, such as earthquakes, tidal waves, and vibrations. Loose saturated sands continue to present problematic ground conditions with disastrous implications. Problems may initiate as liquefaction upon ground's seismicity (Ishihara et al. [27], Chian et al. [28], Ardeshiri-Lajimi et al. [29]). Liquefaction can also cause damage as flow upon static or monotonic loading (Yang and Wei [30]). Static loading has a significant role in the commencement of liquefaction as well as the post-liquefaction flow slides in some practices (Kramer and Seed [31], Hight et al [32]). The static shear stress in the soil can be the driving force of flow slides, after the initiation of liquefaction (Ishihara [27]). Dense sand typically shows dilative volume changes at low confining pressures as stress levels approach failure. This stress-dependent transition, from an initial compressive to dilative behavior, takes place along a 'phase transformation' line under undrained conditions on the stress space. The location of the phase transformation line is dependent on minor and intermediate principal stresses and the sand's relative density (Lade and Ibsen [33]). On the q-p' space, phase transformation occurs on the effective stress

Table 2. Reported list of conducted tests

Test No.	Sand type	$P'c$ (kPa)	$\alpha°$	b	e	D_r %
1	UL	200	15	0.5	0.681	43
2	UL	200	30	0.5	0.682	42
3	UL	200	60	0.5	0.685	41
4	UL	200	15	1	0.688	40
5	UL	200	30	1	0.681	43
6	UL	200	60	1	0.683	42
7	F 161	200	15	0.5	0.723	46
8	F 161	200	30	0.5	0.73	44
9	F 161	200	60	0.5	0.725	45
10	F 161	200	15	1	0.727	45
11	F 161	200	30	1	0.733	43
12	F 161	200	60	1	0.738	41
13	LB	200	15	0.5	0.71	41
14	LB	200	30	0.5	0.708	42
15	LB	200	60	0.5	0.705	42
16	LB	200	15	1	0.702	43
17	LB	200	30	1	0.701	44
18	LB	200	60	1	0.709	41
19	F 131	200	15	0.5	0.8	46
20	F 131	200	30	0.5	0.812	42
21	F 131	200	60	0.5	0.805	45
22	F 131	200	15	1	0.809	43
23	F 131	200	30	1	0.811	43
24	F 131	200	60	1	0.815	41

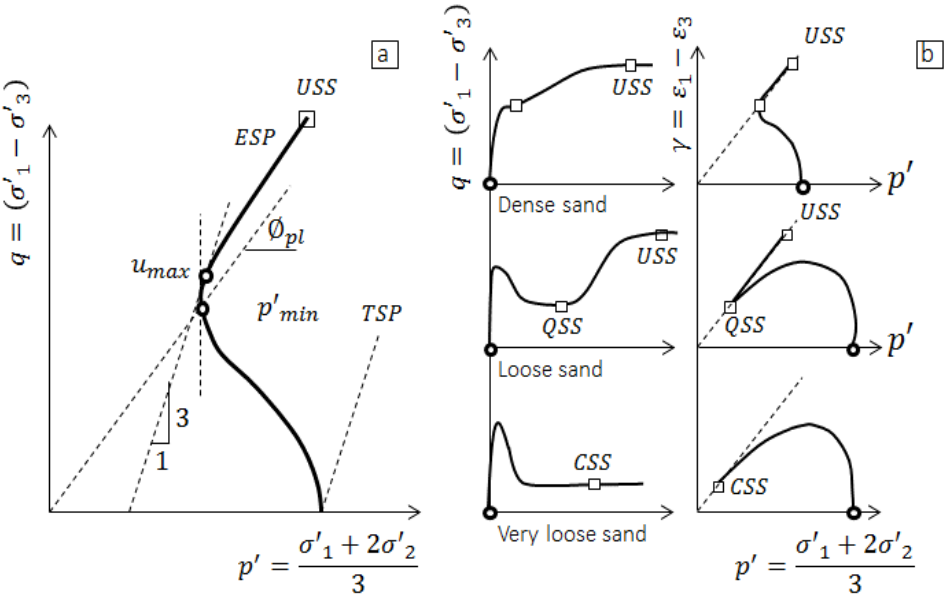

Fig. 8. (a) Phase transformation state during undrained shearing of sand; (b) Steady states during undrained shearing of sand (Modified based on Yoshimine and Ishihara [8]).

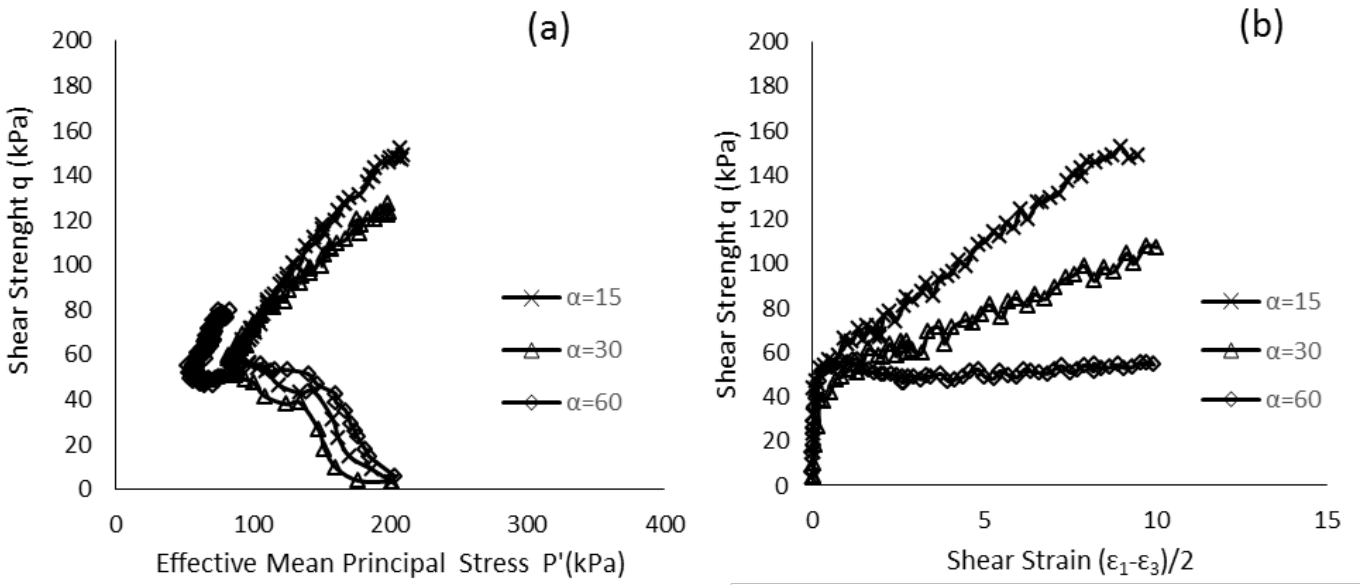

Fig. 9. (a) Stress path and (b) stress-strain curves in Urmia Lake sand in p'= 200 kPa and b=0.5.

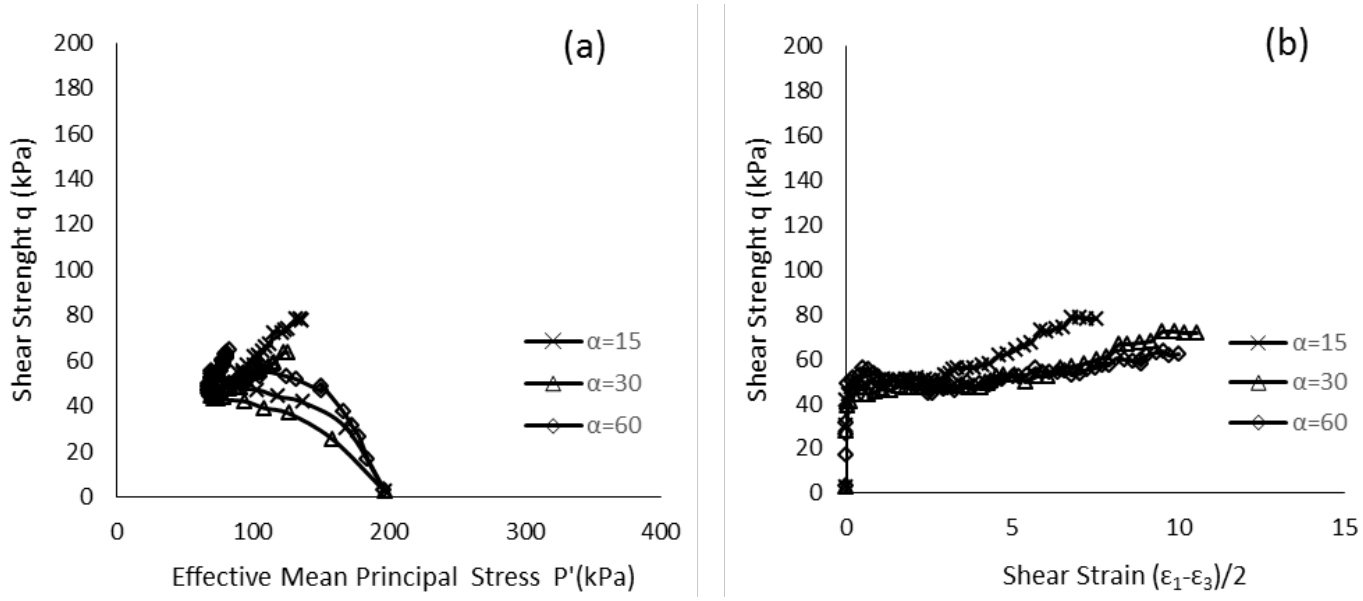

Fig. 10. (a) Stress path and (b) stress-strain curves in Urmia Lake sand in p'= 200 kPa and b=1.

path and where the stress path changes in direction i.e. axis point of curvature, where the effective mean normal stress (*p'*) reaches a minimum value (Fig.8a). Taking 'steady state' as the state of deformation under constant stress components Vaid and Sivathayalan [34]; Yoshimine et al. [35]; Yoshimine and Ishihara [36]), the point of phase transformation can be regarded as a 'steady state'. This state is broadly referred to as the quasi-steady-state (QSS), where post-peak deformations appear under constant effective mean stress p'. The QSS is followed by the ultimate steady state (USS). Unlike dense sands, in loose sands under low confinement levels, at the point of phase transformation the QSS occurs at minimum shear stress (Figure 8b - also see Yoshimine et al. [36]). A course of strain hardening will normally follow the QSS unless sand is at reasonably large levels of initial effective confining pressures (or is at a very loose state whereby confining pressure turns out to be relatively large). In this case, no post-peak hardening develops, and the minimum stress state evolves into the critical steady-state (CSS).

3.2. The Stress-Strain and Stress Paths Diagrams:

As dry pluviation is used as the sampling method in this study, the samples obtained are classified as sands with moderate to lose density using this method. Fig.9 to 16 show

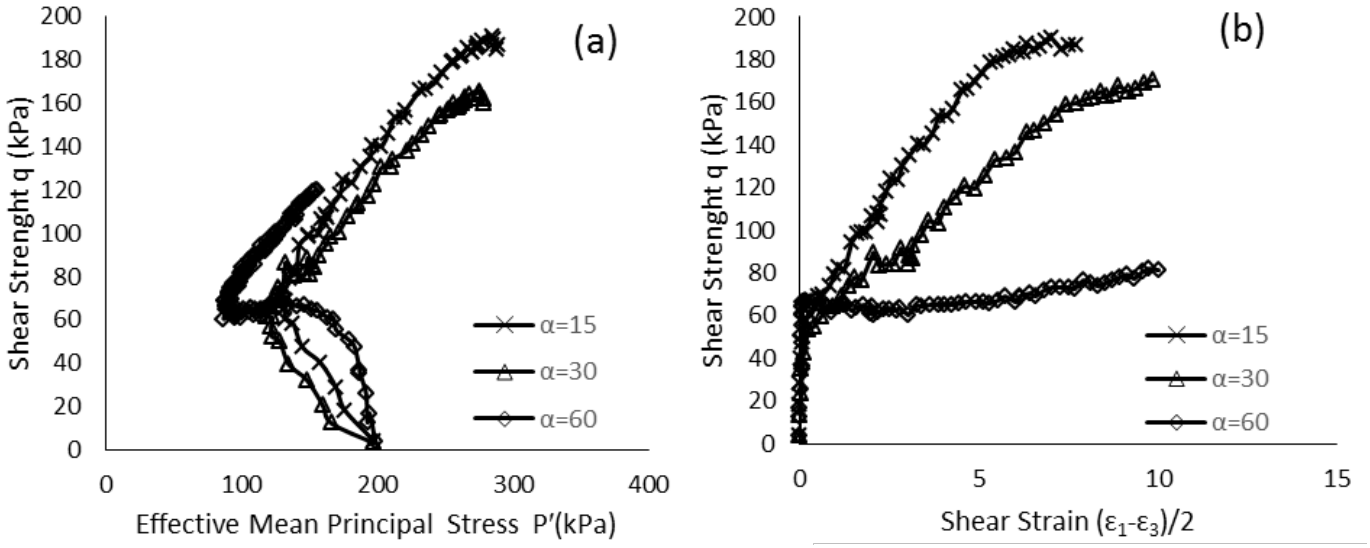

Fig. 11. (a) Stress path and (b) stress-strain curves in Firoozkuh 161 sand in p'= 200 kPa and b=0.5.

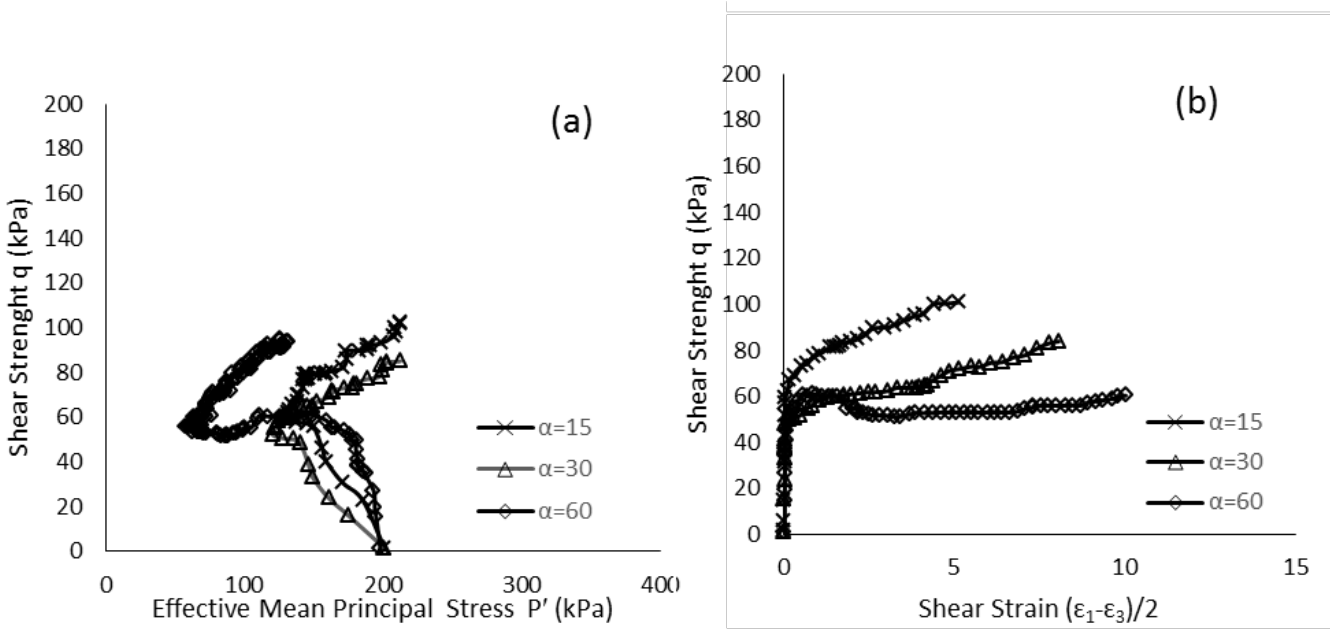

Fig. 12. (a) Stress path and (b) stress-strain curves in Firoozkuh 161 sand in p'= 200 kPa and b=1.

the results of the experiments presented as stress-strain and stress path diagrams. In these experiments, the inclination angle of the major principal stress (α) was changed from 15 to 60 degrees and the experiments were conducted in two intermediate principal stress ratios of 0.5 and 1. Fig.9 and 10 show the diagrams of Urmia Lake (UL). It is observed by considering the diagrams of the Urmia Lake sands that in 15˚ and 30˚ of α, the sand behavior during cutting is non-flow (NF) and hardening, and the behavior of the sand is changed and transformed into a limited-flow (LF) and softener by increasing α to 60˚, there is the same trend in Firoozkuh sand No.161 (Fig. 11 and 12). Increasing the amount of b from 0.5 to 1 in both UL and F161 sands causes a significant decrease in the undrained strength of the samples and changes the

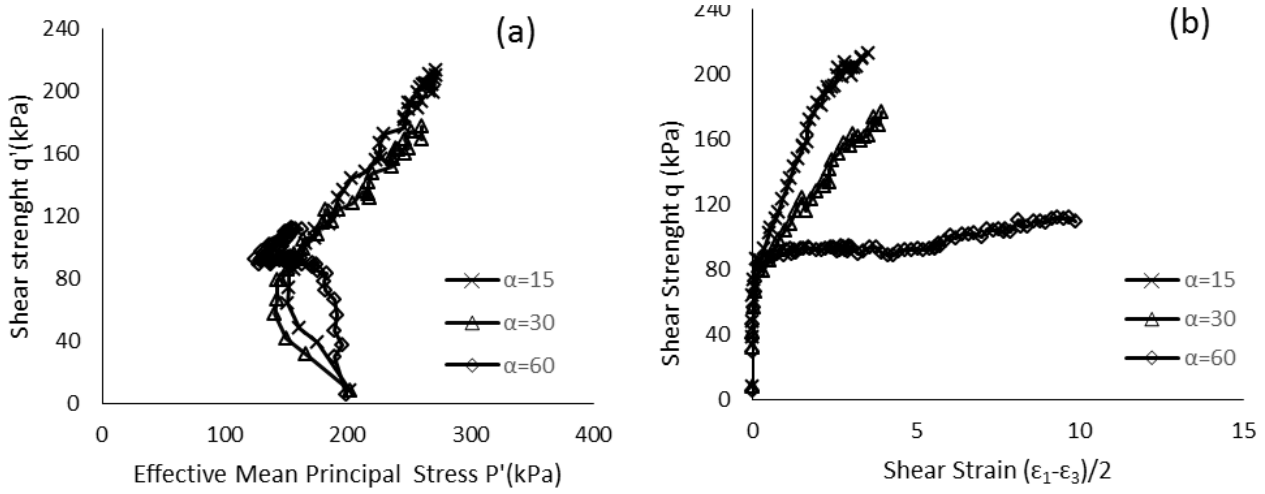

Fig. 13. (a) Stress path and (b) stress-strain curves in Leighton Buzzard sand in p'= 200 kPa and b=0.5.

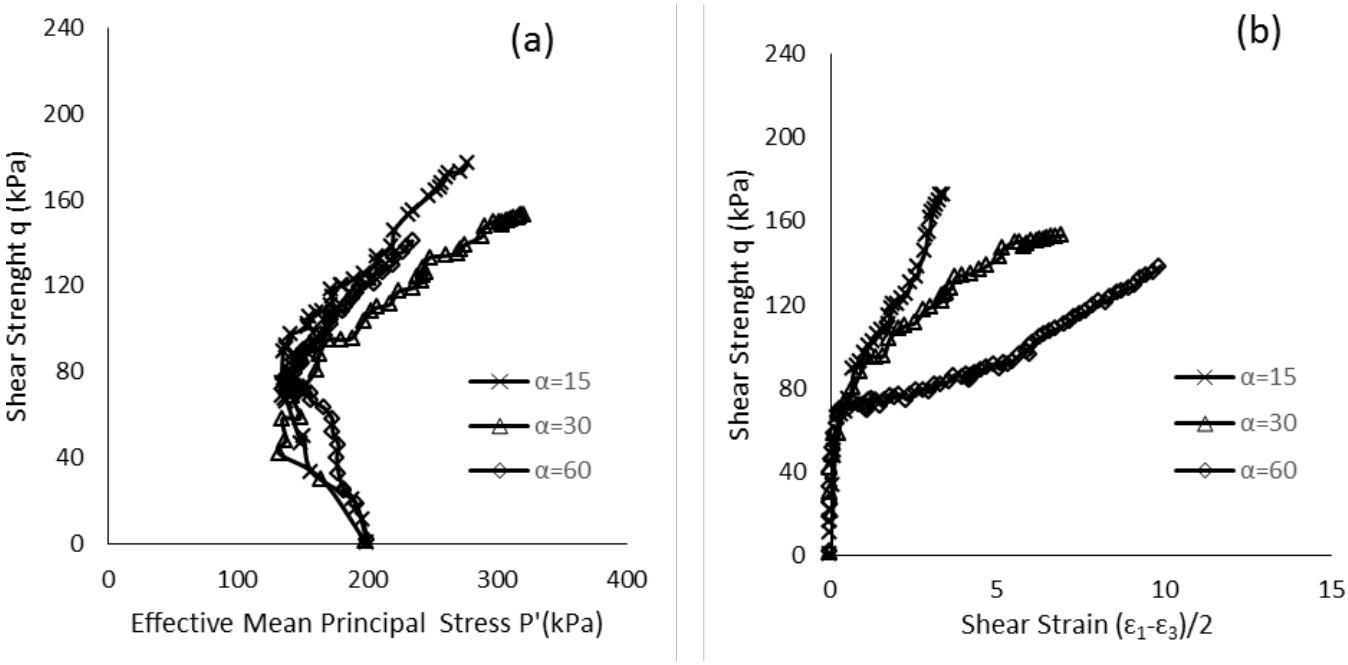

Fig. 14. (a) Stress path and (b) stress-strain curves in Leighton Buzzard sand in p'= 200 kPa and b=1.

behavior of the samples to the fully- softening behavior. This is generally in agreement with previous findings (Shibuya et al. [37]) studied the influence of b-value on the undrained response of medium loose Ham River Sand using HTCA testing apparatus. The behavior of LB and F131 sands in all angles of the major principal stress (α) and the intermediate principal stress ratio (b) are quite hardening and dilative and only the undrained strength of the samples is decreased by increasing α and b and there is no change observed in the behavior in this type of sands (Fig.13-16).

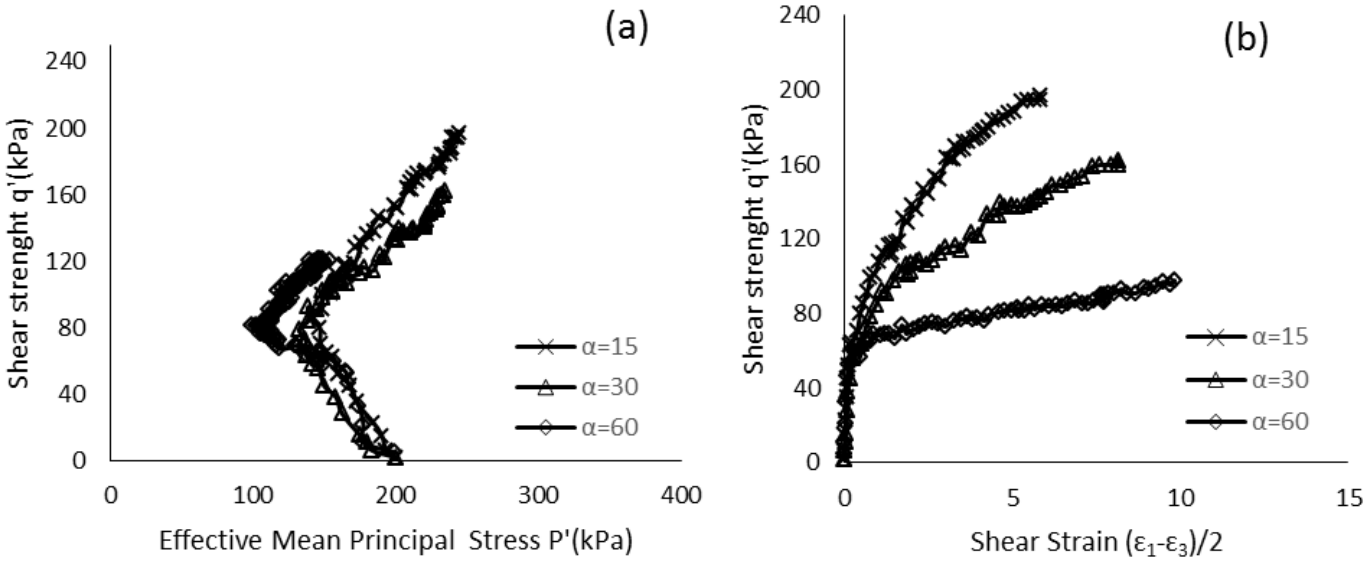

Fig. 15. (a) Stress path and (b) stress-strain curves in Firoozkuh 131 sand in p'= 200 kPa and b=0.5.

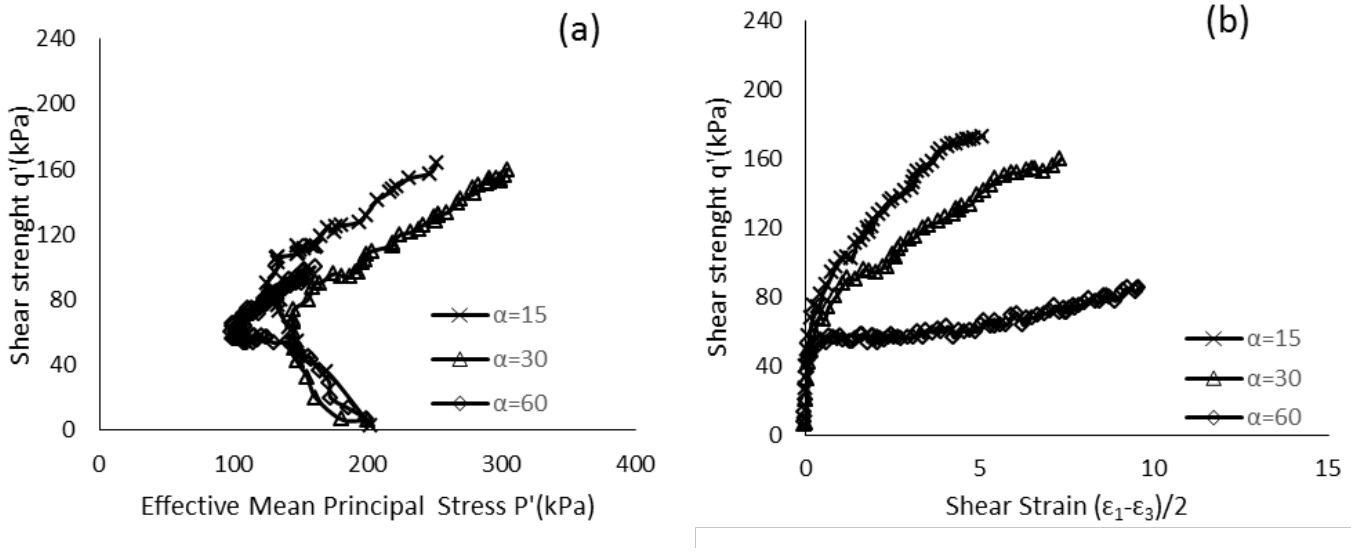

Fig .16. (a) Stress path and (b) stress-strain curves in Firoozkuh 131 sand in p'= 200 kPa and b=1.

Fig.17 shows the undrained shear strength of steady-state (q_{ss}) of the samples at the three inclination angles of the major principal stress (α) and two intermediate stress ratios of 0.5 and 1. The tests related to the 0.5 and 1 intermediate stress ratio of these samples indicate that the highest difference between the shear strength of the steady-state of samples is related to F131 sand and the lowest amount is for the Urmia Lake sand, meaning that, there is a significant decrease in undrained shear strength of steady-state of the samples in F131 sand with increasing α from 15° to 60° compared to other sands. Accordingly, it can be said that the effect of anisotropy on coarse sands is higher than fine sands. Considering these diagrams, it is observed that the undrained shear strength of all four types of sand is decreased by increasing α and b. Findings are in good agreement with early attempts in Yoshimine and Ishihara [8] and Bahadori et al. [12] on Toyoura and Firoozkuh sands.

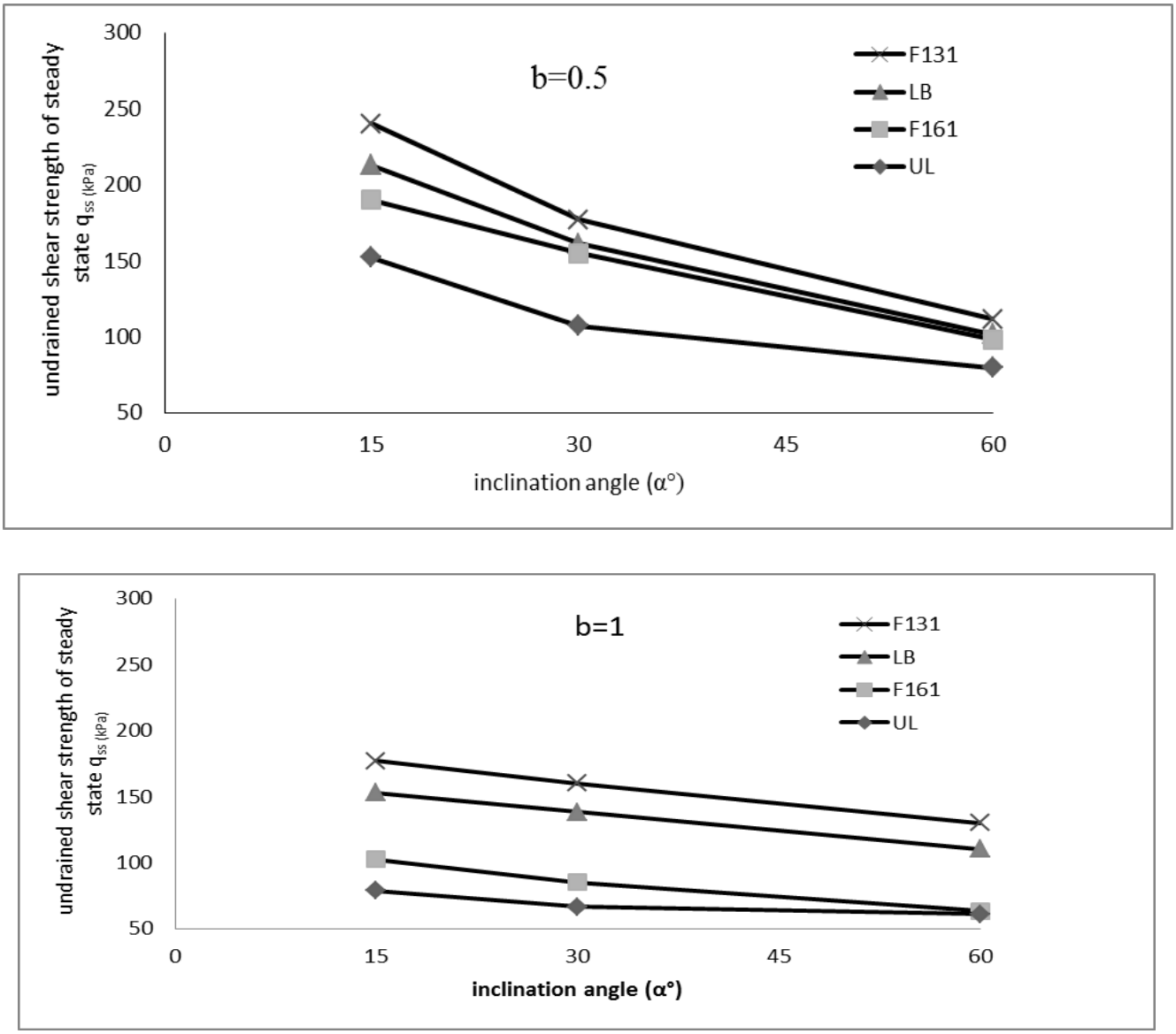

Fig.17. Undrained shear strength of steady-state (qss) of the samples at the three inclination angles (α) and two intermediate stress ratios (b) of 0.5 and 1.

3.3. Effect of particle size

In this research, the mean grain diameter (D50) is used as a characteristic parameter of soil grain size to examine the effect of grain size on the anisotropic behavior of saturated sands. Fig.19 shows the relationship between the mean diameters of grains (D50) of four types of sand with a normalized shear strength of steady-state (q_{ss} / p_c') of the samples. These diagrams represent that the undrained shear strength of the steady state of the samples as been increased by increasing the grain size. Examining these diagrams in detail represents that the distance between the diagrams of $\alpha = 15^{\circ}$ and $\alpha = 30^{\circ}$ with $\alpha = 60$ is increased by increasing the sand size, and the difference in the value of un-drained shear strength of sand samples is increased. Therefore, it can be concluded that the undrained shear strength of steady-state of sand samples with coarse particles, with increasing the inclination angle of the major principal stress (α), changes more than that of sand particles with fine particle size. This matter shows that the effect of anisotropy in coarse sand samples is higher than the fine sand samples.

3.4. Effect of particle shape

In this study, the sphericity and roundness parameters are used as dimensionless parameters of the particle shape to examine the effect of sand shape on the anisotropic behavior of saturated sands. Sand samples are used to compare, that are closer to each other in physical characteristics to improve the relationship between shape and strength parameters and

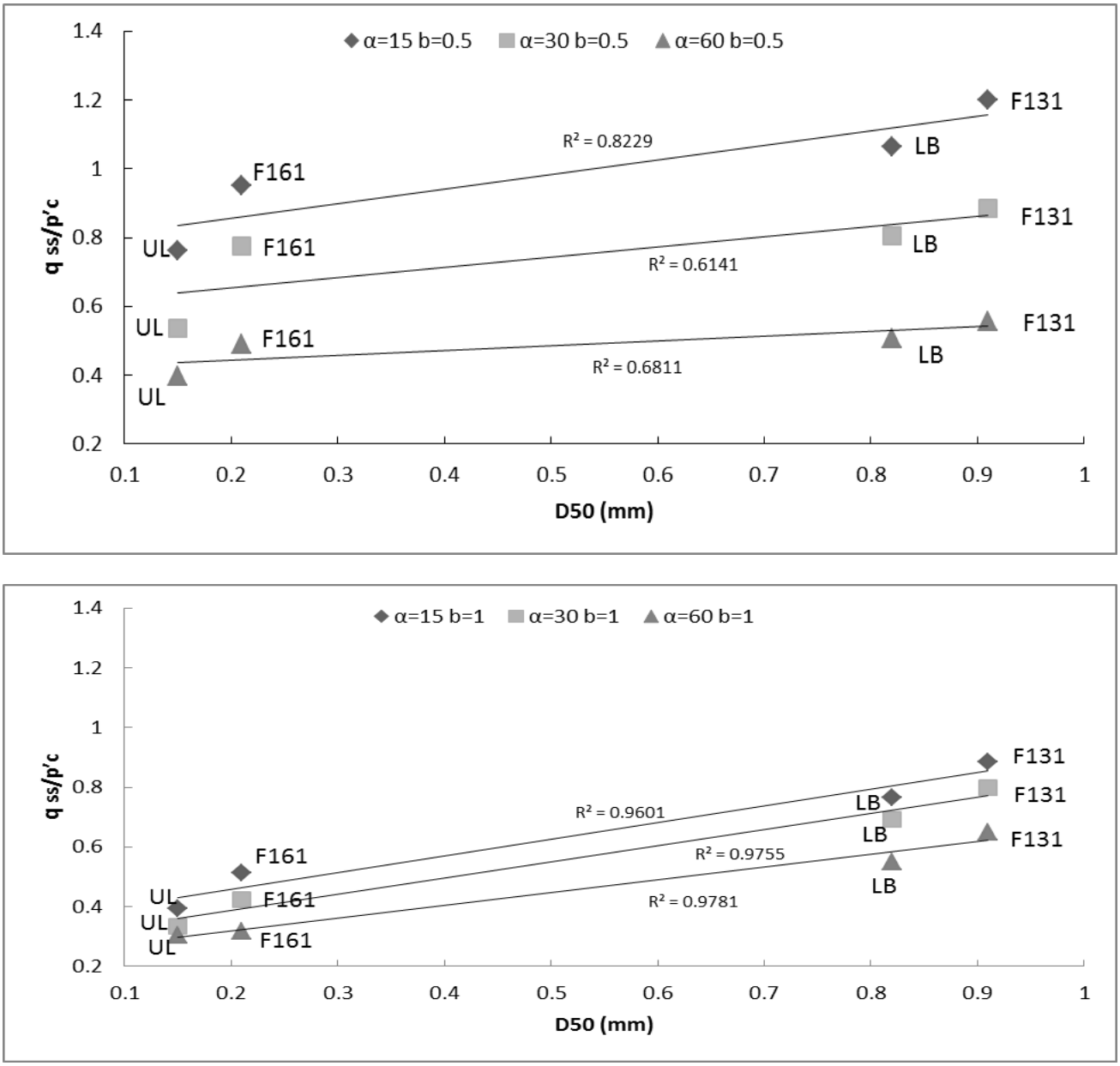

Fig. 18. Relation between normalized shear strength of steady-state of the samples (q_{ss}/p'_c) and mean grain diameter (D50).

to reduce the effect of other variables, therefore, the results of UL sand tests are compared to sand F161 (as fine sand) and LB sand with F131 sand (as coarse sand).

According to the microscopic images of UL sand and F161 (Fig.1) and the results from the 2D image analysis (Table 1), the roundness parameter of the UL sand due to its natural origin is twice more than the F161 sand. It means that the F161 sand grains are more angular. Fig.19 shows the relationship between the roundness parameter and the normalized shear strength steady states of the UL and F161 sands in the intermediate principal stress ratio of 0.5. The results of experiments conducted that undrained shear strength of the samples at all three inclination angles of the major principal stress (α) is reduced by increasing the sand roundness, and the normalized shear strength of the steady-state points of both sand types is decreased by increasing the value of α. The significant point is that the shear strength of the F161 sand, despite having a larger particle size than the UL sand is decreased highly by increasing α from 30° to 60°, and it has a very low strength difference with the UL sand. This indicates that in F161 sand, the decrease of strength in $\alpha = 60^\circ$ is much higher than the UL sand, and the anisotropy effect on the F161 sand, which is more angular, is higher than the UL sand.

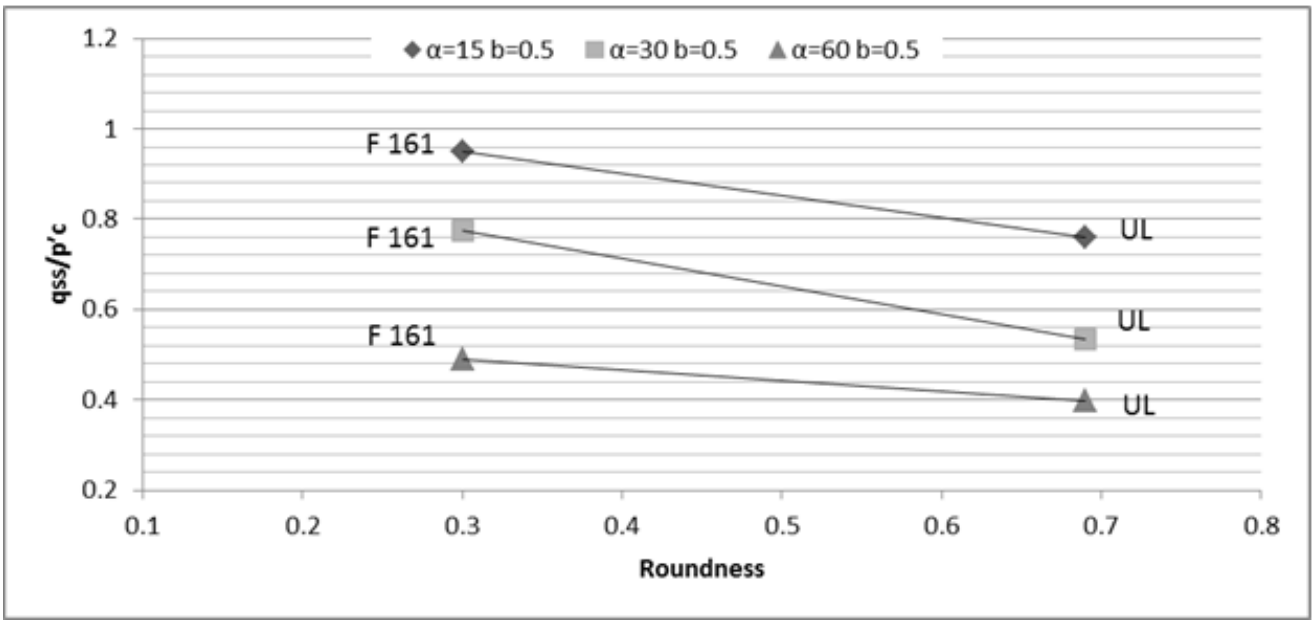

Fig. 19. Relation between the roundness parameter (R) and the normalized shear strength of the UL and F161 sands in the intermediate principal stress ratio of 0.5.

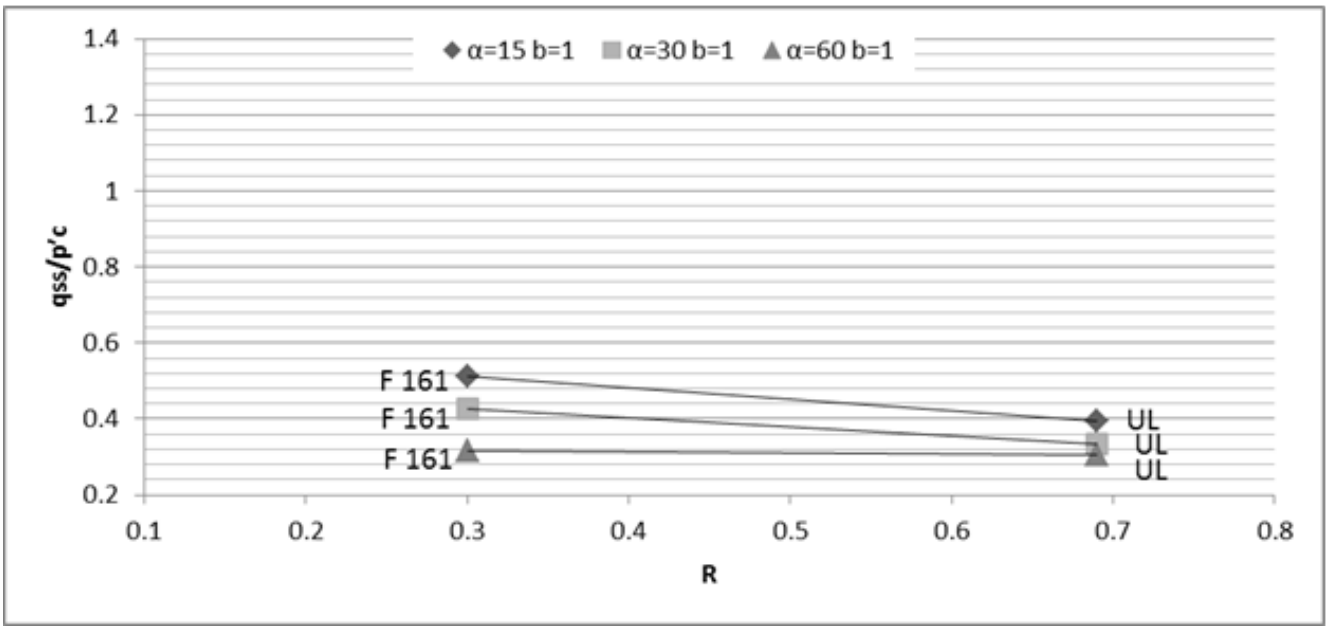

Fig. 20. Relation between the roundness parameter (R) and the normalized shear strength of the UL and F161 sands in the intermediate principal stress ratio of 1.

There is a significant reduction of shear strength in both UL and F161 sand samples by increasing the intermediate principal stress ratio (*b*) from 0.5 to 1(Figure 20). The behavior of samples tested with the intermediate principal stress ratio of $b = 1$ are very similar to samples tested with $b = 0.5$, in a way that the shear strength of the steady-state of the UL sand in all three inclination angles of the major principal stress of 15°, 30°, and 60° are very near to the F161 sand, which concludes that the anisotropy effect in the Urmia Lake sand is more observable than the F161 sand. Therefore, it can be explained that the anisotropy effect is decreased by increasing the grain's roundness.

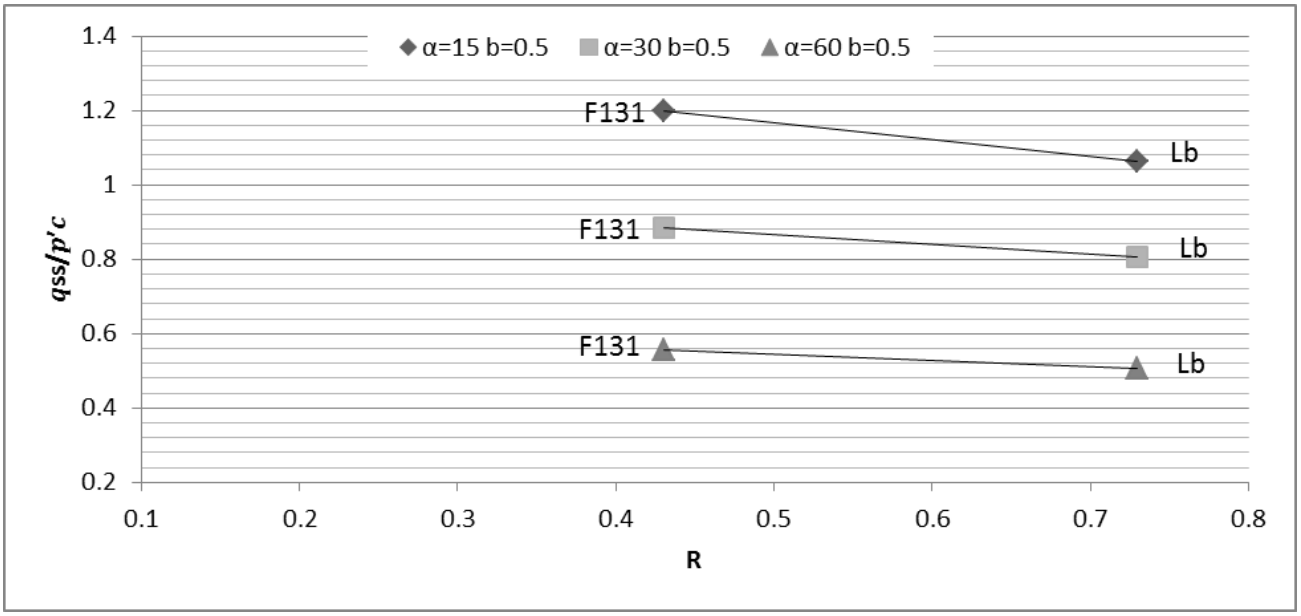

Fig. 21. Relation between the grain roundness parameter (R) and the normalized shear strength of the steady-state of LB and F131 sands in the intermediate principal stress ratio of 0.5.

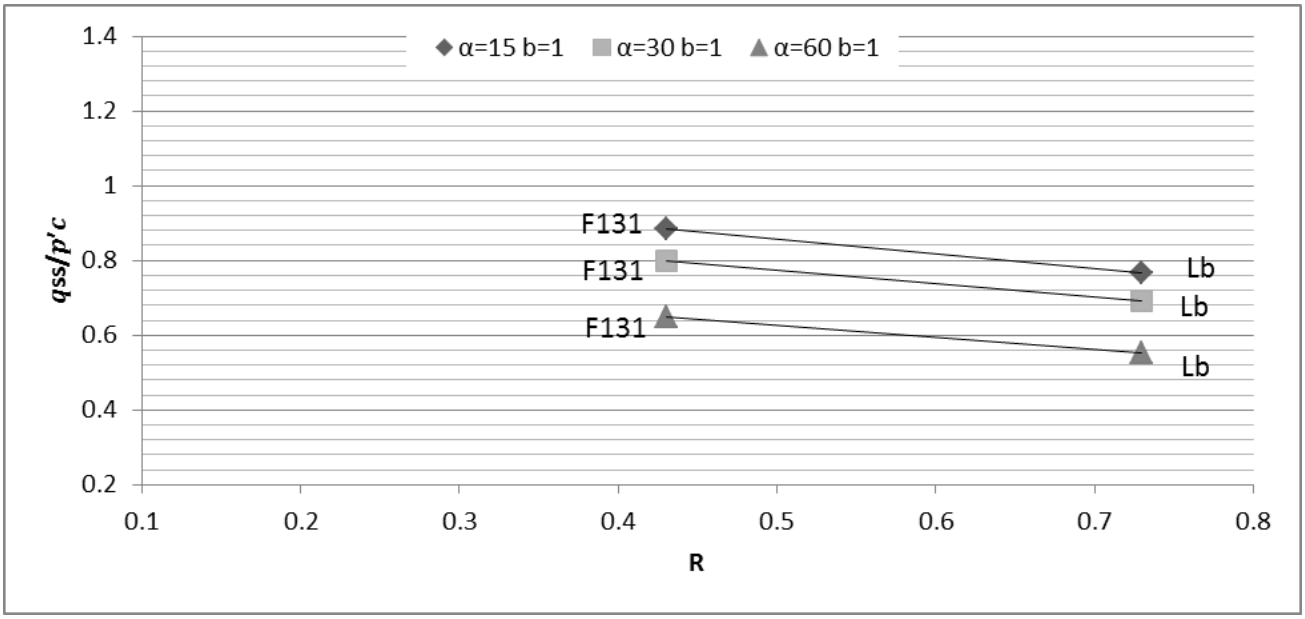

Fig. 22. Relation between the grain roundness parameter (R) and the normalized shear strength of the steady-state of LB and F131 sands in the intermediate principal stress ratio of 1.

Fig.21 shows the relationship between the grain roundness parameter (R) and the normalized shear strength of the steady-state of LB and F131 sands in the intermediate principal stress ratio of 0.5. The diagrams of LB and F131 sands show that in these sands, as Urmia Lake sands and F161, the normalized shear strength of the steady state of the samples is reduced by increasing the roundness of sands. But unlike the results in the fine grain sands, the anisotropy effect in the steady-state of the samples is reduced by increasing the roundness of the grains and there is a significant difference between the shear strength of the steady-state of the samples in various α in the round LB sand such as angular F131 sand. The same trend is repeated in tests with an intermediate principal stress ratio (*b*) of 1 (Fig.22).

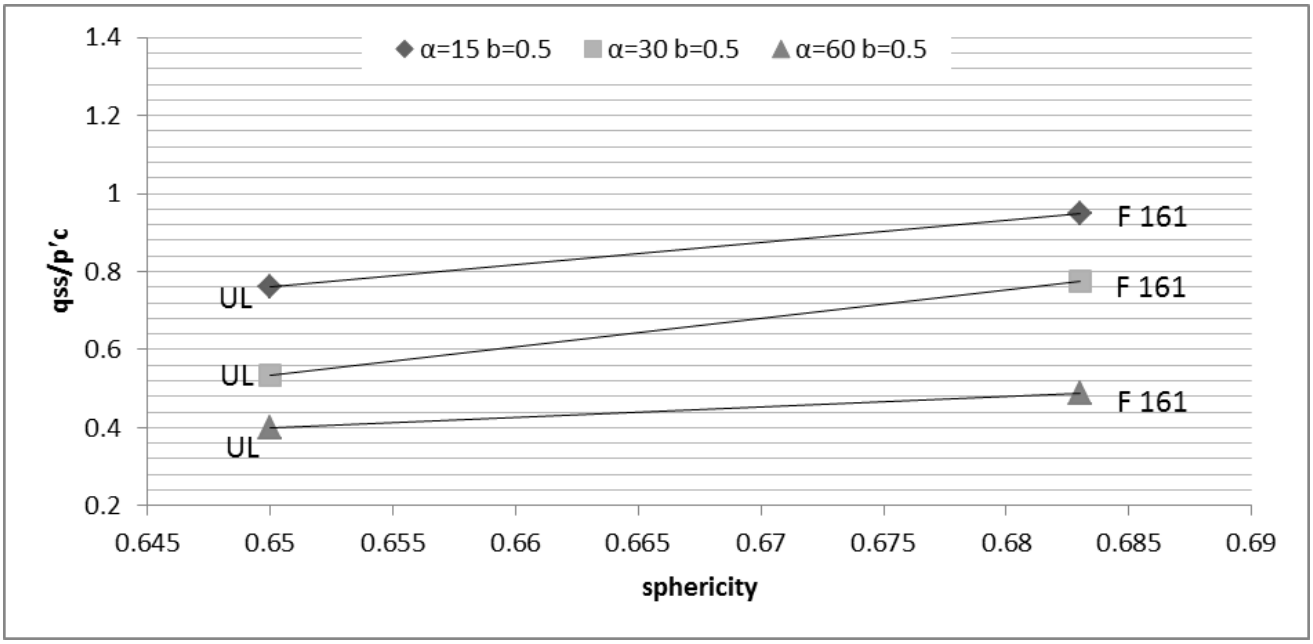

Fig. 23. Relation between grain sphericity parameter (S) and normalized shear strength of the steady-state of UL and F161 sands in the intermediate principal stress ratio of 0.5.

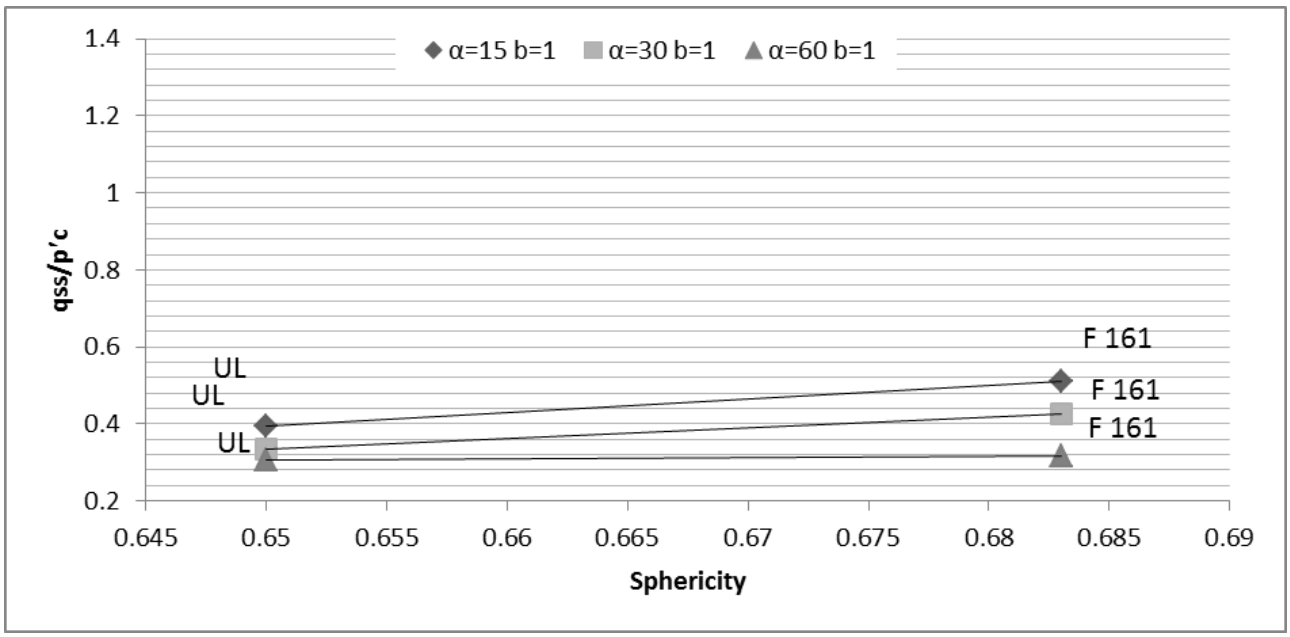

Fig. 24. Relation between grain sphericity parameter (S) and normalized shear strength of the steady-state of UL and F161 sands in the intermediate principal stress ratio of 1.

The results of two-dimensional analysis of microscopic images of Urmia Lake and F161 sands explain that the mean sphericity of F161 sand grains is higher than Urmia Lake sand. It is realized by paying a little attention to the microscopic images of these sands that the Urmia Lake sand grains are slightly longer and more cylindrical than F161 sand, which reduced the mean grain sphericity (Fig.2). Fig.23 and 24 show the relationship between grain sphericity parameter and normalized shear strength of the steady-state of UL and F161 sands in the intermediate principal stress ratio of 0.5 and 1. The normalized shear strength of the steady-state of the samples has been increased in all three α by increasing the sphericity of grains. This indicates that the shear strength of the sand samples is increased by increasing the sphericity of grains. It will be clear by paying a little attention to these diagrams that the difference in the undrained shear strength

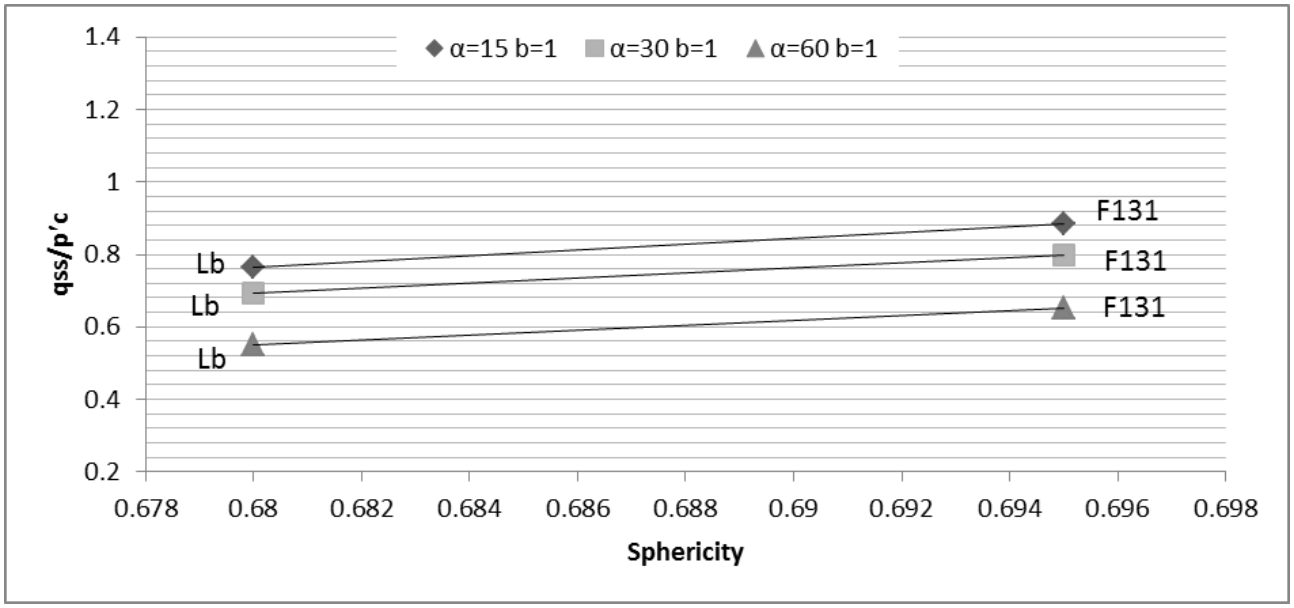

Fig. 25. Relation between grain sphericity parameter (S) and normalized shear strength of the steady-state of LB and F131 sands in the intermediate principal stress ratio of 0.5.

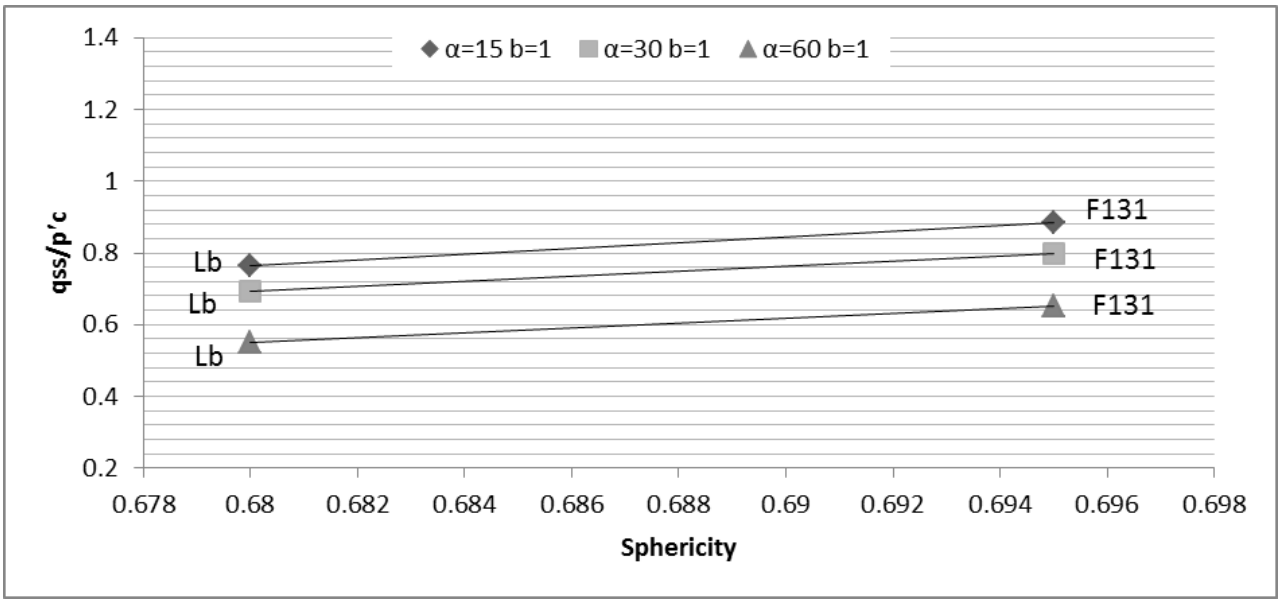

Fig. 26. Relation between grain sphericity parameter (S) and normalized shear strength of the steady-state of LB and F131 sands in the intermediate principal stress ratio of 1.

of the samples from the Firoozkuh sand has been increased by increasing α from 15˚ to 60˚. Hence, it can be concluded that the more sphere is the sandy grains, the anisotropy effect is more on them.

Fig.25 and 26 show the relationship between the sphericity parameter of grains (*S*) and normalized shear strength of the steady-state of LB and F131 sands. Moreover, the anisotropy effect is increased in these sands by increasing the sphericity of grains (*R*), and the difference between the undrained shear strength of the samples is increased by increasing the inclination angle of the major principal stress (*α*).

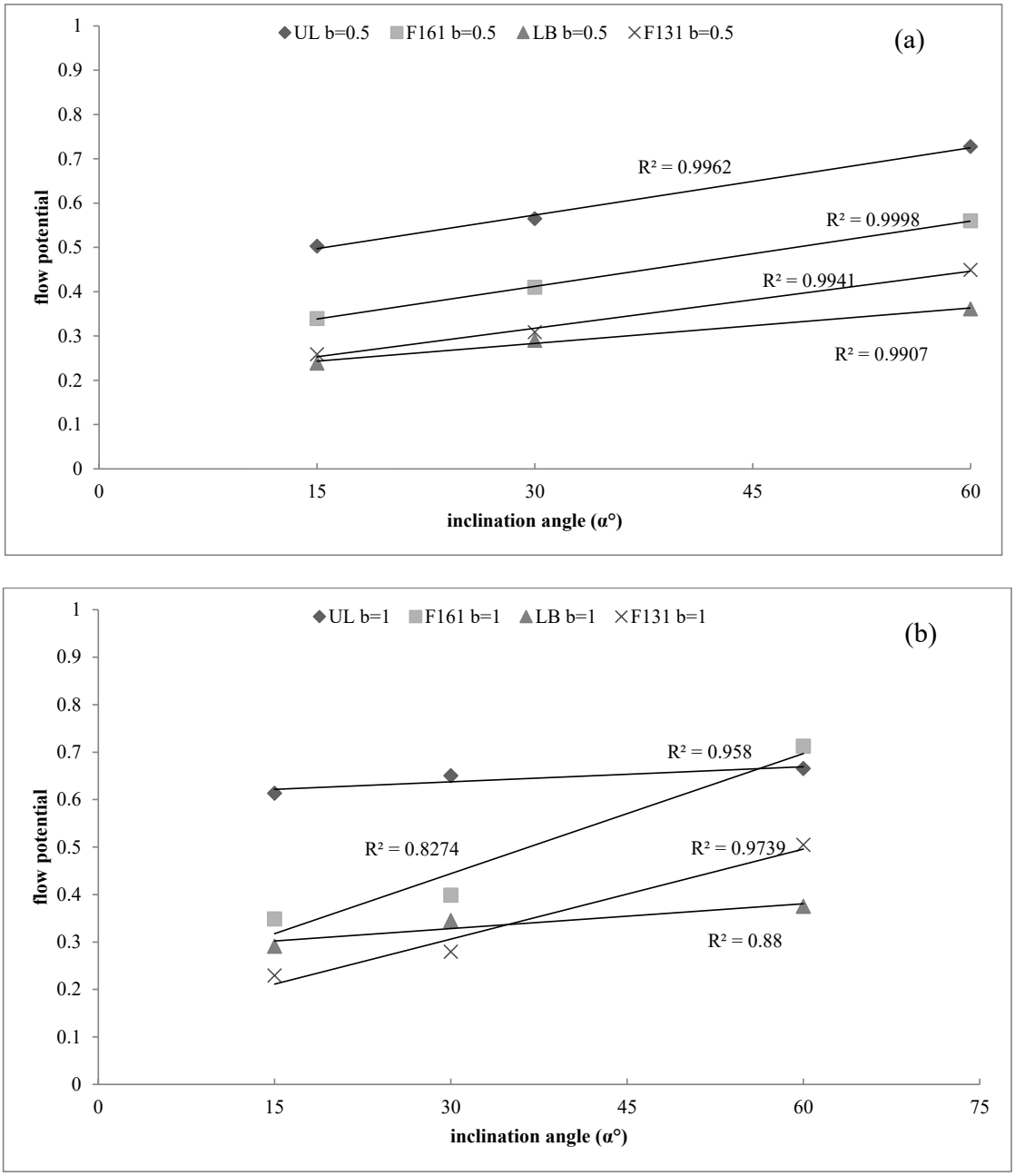

Fig. 27. The effect of inclination angle on the flow potential.

4- Further discussions

4.1. Flow potential

The observations on strain softening and contraction in the sand and their association with anisotropy necessitate defining a state index to measure the softening (i.e. flow) potential. Yoshimine and Ishihara [36] suggested the use of u_f, the maximum excess pore water pressure ratio, as a softening factor. The u_f index (i.e. herein known as flow potential) is controlled by stress conditions in sand during both initial and shearing stages, and by the intermediate principal stress and direction of principal stresses. Eq. (9) formulates the flow potential as a function of P'_{PT} (the mean effective pressure at the point of phase transformation) and P'_c (mean isotropic confining pressure).

$$u_f = 1 - \frac{P'_{PT}}{P'_c} \tag{9}$$

It should be noted that the flow potential u_f is not an index of property fixed by initial conditions alone, but is strongly affected by the stress conditions during deformation. It can be considered as a softening index. Fig.27a shows the relationship between the inclination angle of the major

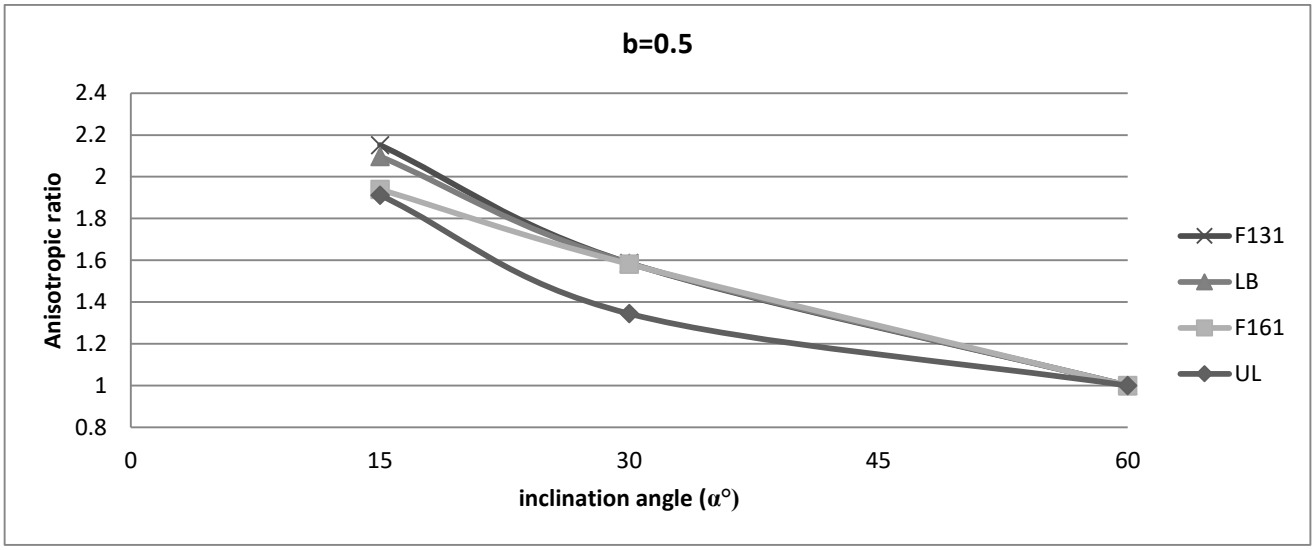

Fig. 28. Effect of inclination angle α° on the anisotropic ratio at intermediate principle stress of 0.5.

principal stress and the flow potential in samples tested with the intermediate principal stress ratio of 0.5. All four types of sand show that the potential flow rate is increased by increasing the inclination angle of the major principal stress from 15° to 60°, so that, the un-drained strength of the samples is reduced by increasing the inclination angle of the major principal stress (α) and the behavior of samples becomes softening. These diagrams indicate that the flow potential is reduced by increasing the particle size. However, this trend is not observed in F131 sand. Although the size of the Firoozkuh sand particles is larger than the LB sand, it is clear that the flow potential in the F131 sand is more than LB sand. This phenomenon is caused by the behavior of the sand and the increased amount of pore water pressure formed in the sand. Therefore, it can be said that the production of pore water pressure in the F131 and is much higher than the LB sand, which reduces the mean principal stresses at the phase transformation point P'_{PT} and increases the potential flow of the F131 sand. Figure 19b shows the relationship between the inclination angle of the major principal stress and the flow potential in samples that are tested with the intermediate principal stress ratio of 1. Examining these diagrams specified that the diagram slope of the F161 and F131 sand grains, which have less roundness than the UL and LB sand grains, is much higher. This result indicates that by increasing the inclination angle α, the flow potential in sands with more angular grains is much higher than the sand with round grains.

The flow potential in all four types of sand is increased by increasing the inclination angle of the major principal stress from 15° to 60° which means that the undrained shear strength of the samples is decreased by increasing the inclination angle of the major principal stress (α) and the behavior of the samples become more softening. In the more angular sands, the flow potential is increased more than that of the rounded sands by increasing the inclination angle of the major principal stress.

4.2. Anisotropy Ratio

Eq. (10) shows the anisotropic ratio parameter as proposed by Zarei et al. [1]. This parameter evaluates the anisotropy effects of samples in different values of inclination angles α.

$$AR = \frac{q_{ss(\alpha^\circ)}}{q_{ss(\alpha^\circ=60)}} \quad (1)$$

$q_{ss(\alpha^\circ)}$ and $q_{ss(\alpha^\circ=60)}$ represent the undrained shearstrength of steady-state at arbitrary α° and $\alpha^\circ=60^\circ$, respectively. Fig.28 and 29 reveals the variations of AR versus different values of α°. According to these figures, the AR values of F131 sand have the most variation between other sands in both intermediate principal stress ratios. It means that the anisotropy effects increase by increasing the grain sizes.

5. CONCLUSIONS

From the series of un-drained torsional tests conducted by hollow cylindrical torsional shear apparatus on four different grains of sand with different particle sizes and morphological characteristics, the following major conclusions are drawn from the present work.

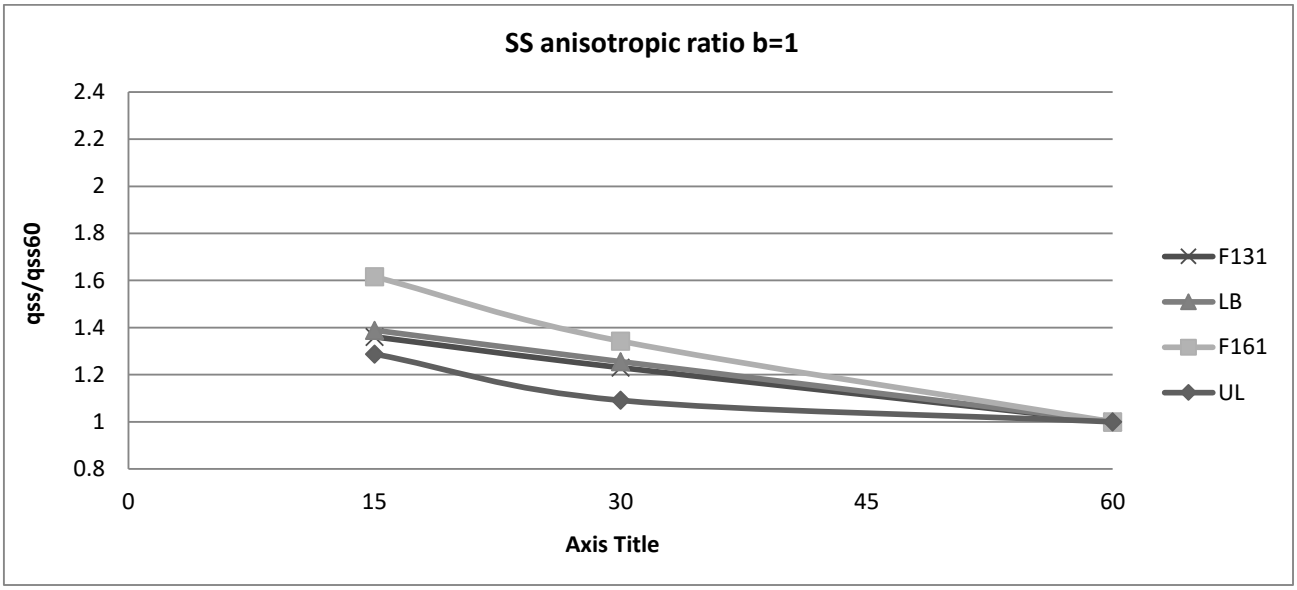

Fig. 29. Effect of inclination angle α° on the anisotropic ratio at intermediate principle stress of 1.

- In fine-grain sand samples (UL, F161), the behavior at α of 15° and 30° was completely non-flow and hardening, and the behavior of the sands was changed and became limited flow (LF) and softening by increasing α to 60°, while in coarse grain sands (LB, F131) at all applied inclination angles the behavior of the samples is quite hardening and non-flow. And by increasing α, there is no behavior variation from non-flow and hardening to flow and softening.
- In fine-grain sand samples (UL, F161), the behavior at α of 15° and 30° was completely non-flow and hardening and the behavior of the sands was changed and became limited flow (LF) and softening by increasing α to 60°, while in coarse grain sands (LB, F131) at all applied inclination angles the behavior of the samples is quite hardening and non-flow. And by increasing α, there is no behavior variation from non-flow and hardening to flow and softening.
- In fine-grain UL and F161 sands, there is a significant decrease in un-drained shear strength of the samples caused by the increase of b from 0.5 to 1, and the behavior of samples changed from non-flow to flow behavior with limited deformation. But the behavior of the LB and F131 sands is completely non-flow and there are no changes in behavior in coarse grain sands by increasing the value of b, despite the reduction of the shear strength of samples.
- The experiment results of sand samples express that the highest difference between the shear strength of the steady-state of samples is related to F131 sand and the least amount is related to Urmia Lake sand, which means that there is a significant decrease in un-drained strength of the steady-state of the samples compared to other sands in F131 sand by increasing α from 15° to 60°. Hence, it can be said that the anisotropy effect on the shear strength of the steady-state of coarse grain sands is more than fine grain sands.
- The results of experiments conducted on fine sand samples (UL and F161) explain that the undrained shear strength of samples is reduced by increasing the roundness of grains (R)and the difference of shear strength in different α between samples of F161 sand is more than UL sand. It means that the anisotropy effect in angular sands is higher than rounded sand, and the anisotropy effect is decreased by increasing the grain size.
- In coarse grain sands (LB, F131) as fine-grain sands. The undrained shear strength of the samples is reduced by increasing the grain roundness (*R*). But the results of experiments conducted on these sands show that the roundness of grains has no much effect on the behavior and undrained shear strength of the coarse grain sands.
- The results of the experiments on all four types of sand show that their undrained shear strength is increased by increasing the sphericity of the sand particles, it means that if there are less cylindrical shape and long particles in the soil, the soil will have more strength. On the other hand, the more the sphericity of the sand particles, the greater is the difference between their undrained strength in different *α*, which means that the anisotropy effect is also increased by increasing the sphericity parameter.

Notation

α^0	Direction of the major principal stress axis relative to the vertical direction
b	Intermediate principal stress parameter
D_{50}	Mean particle size
e_{min}, e_{max}	Minimum and maximum void ratio
H	Initial specimen height
HCTA	Hollow Cylinder Torsional Apparatus
r_i, r_o	Inner and outer radius of the hollow cylinder specimen
$P'c$	Mean isotropic effective confining stress
e_c	Void ratio after isotropic consolidation
p'_{PT}	Mean effective stress at phase transformation
$(\varepsilon_1-\varepsilon_3)/2$	Deviatoric axial strain
q_{peak}	Peak strength
q	Deviatoric stress
p'	Mean effective stress
σ_1, σ_2, σ_3	Mean major, intermediate and minor total principal stress
ε_1, ε_2, ε_3	Principal strain
u_f	Flow potential index

References

[1] C. Zarei, H. Soltani-Jigheh, K. Badv, Effect of Inherent Anisotropy on the Behavior of Fine-Grained Cohesive Soils, International Journal of Civil Engineering, 17(6) (2019) 687-697.

[2] K. Ishihara, I. Towhata, Sand response to cyclic rotation of principal stress directions as induced by wave loads, Soils and foundations, 23(4) (1983) 11-26.

[3] D. Pradel, K. Ishihara, M. Gutierrez, Yielding and flow of sand under principal stress axes rotation, Soils and Foundations, 30(1) (1990) 87-99.

[4] T.B. Pradhan, F. Tatsuoka, N. HORII, Simple shear testing on sand in a torsional shear apparatus, Soils and Foundations, 28(2) (1988) 95-112.

[5] S. Sivathayalan, Y. Vaid, Influence of generalized initial state and principal stress rotation on the undrained response of sands, Canadian Geotechnical Journal, 39(1) (2002) 63-76.

[6] M. Symes, A. Gens, D. Hight, Undrained anisotropy and principal stress rotation in saturated sand, Geotechnique, 34(1) (1984) 11-27.

[7] M. Uthayakumar, Y. Vaid, Static liquefaction of sands under multiaxial loading, Canadian Geotechnical Journal, 35(2) (1998) 273-283.

[8] M. Yoshimine, K. Ishihara, W. Vargas, Effects of principal stress direction and intermediate principal stress on undrained shear behavior of sand, Soils and Foundations, 38(3) (1998) 179-188.

[9] A. Saada, F. Townsend, State of the art: laboratory strength testing of soils, in: Laboratory shear strength of soil, ASTM International, 1981.

[10] Z. Yang, X. Li, J. Yang, Undrained anisotropy and rotational shear in granular soil, Géotechnique, 57(4) (2007) 371-384.

[11] H. Shahnazari, I. Towhata, Torsion shear tests on cyclic stress-dilatancy relationship of sand, Soils and Foundations, 42(1) (2002) 105-119.

[12] H. Bahadori, A. GHALANDARZADEH, I. Towhata, Effect of non plastic silt on the anisotropic behavior of sand, Soils and Foundations, 48(4) (2008) 531-545.

[13] N. Khayat, A. Ghalandarzadeh, M.K. Jafari, Grain shape effect on the anisotropic behaviour of silt–sand mixtures, Proceedings of the Institution of Civil Engineers-Geotechnical Engineering, 167(3) (2014) 281-296.

[14] W. Holz, H. Gibbs, Triaxial shear tests on previous gravelly soils, J Soil Mech Found Div ASCE, 82(867) (1956) 1-867.822.

[15] M. Frederick, Notes on the shape of particles and its influence on the properties of sands, Proc. of the Midland Soil Mechanics and Foundation Engineering Society, (1961) 157-162.

[16] J. Kolbuszewski, M. Frederick, The significance of particle shape and size on the mechanical behaviour of granular materials, in: Proceedings of European conference on the soil mechanics and foundation engineering, 1963, pp. 253-263.

[17] E. Zolkov, G. Wiseman, Engineering properties of dune and beach sands and the influence of stress history, in: Proc. of Sixth Int. Conf. on SMFE, 1965, pp. 134-138.

[18] W. Kirkpatrick, Effects of grain size and grading on the shearing behaviour of granular materials, in: Proceedings of the Sixth International Conference on Soil Mechanics and Foundation Engineering, 1965, pp. 273-277.

[19] N.D. Marschi, C.K. Chan, H.B. Seed, Evaluation of properties of rockfill materials, Journal of the Soil Mechanics and Foundations Division, 98(1) (1972) 95-114.

[20] B. Chattopadhya, S. Saha, Effect of grain size of cohesionless soil on its shear strength characteristics, in: Geomech. 81 Proc. vol. 1, Symposium on Engineering Behaviour of Coarse Grained Soils, Boulders and Rock, 1981, pp. 291-297.

[21] T. Sitharam, M. Nimbkar, Micromechanical modelling of granular materials: effect of particle size and gradation, Geotechnical & Geological Engineering, 18(2) (2000) 91-117.

[22] M.N. Islam, A. Siddika, M.B. Hossain, A. Rahman, M.A. Asad, Effect of particle size on the shear strength behavior of sands, Australian Geomechanics, 46 (2019).

[23] P. Vangla, G.M. Latha, Influence of particle size on the friction and interfacial shear strength of sands of similar morphology, International Journal of Geosynthetics and Ground Engineering, 1(1) (2015) 6.

[24] W. Krumbein, L. Sloss, Stratigraphy and Sedimentation, Soil Science, 71 (1951) 401.

[25] G.-C. Cho, J. Dodds, J.C. Santamarina, Particle shape effects on packing density, stiffness, and strength: natural and crushed sands, Journal of geotechnical and geoenvironmental engineering, 132(5) (2006) 591-602.

[26] P.V. Lade, N.M. Rodriguez, Comparison of true triaxial and hollow cylinder tests on cross-anisotropic sand specimens, Geotechnical Testing Journal, 37(4) (2014) 585-596.

[27] K. Ishihara, Liquefaction and flow failure during earthquakes, Geotechnique, 43(3) (1993) 351-451.

[28] S.C. Chian, K. Tokimatsu, S.P.G. Madabhushi, Soil liquefaction–induced uplift of underground structures: physical and numerical modeling, Journal of Geotechnical and Geoenvironmental Engineering, 140(10) (2014) 04014057.

[29] S. Ardeshiri-Lajimi, M. Yazdani, A. Assadi Langroudi, A Study on the liquefaction risk in seismic design of foundations, Geomechanics and Engineering, 11(6) (2016) 805-820.

[30] J. Yang, L. Wei, Collapse of loose sand with the addition of fines: the role of particle shape, Géotechnique, (2012).

[31] S.L. Kramer, H.B. Seed, Initiation of soil liquefaction under static loading conditions, Journal of Geotechnical Engineering, 114(4) (1988) 412-430.

[32] D. Hight, J. Bennell, B. Chana, P. Davis, R. Jardine, E. Porovic, Wave velocity and stiffness measurements of the Crag and Lower London Tertiaries at Sizewell, Géotechnique, 47(3) (1997) 451-474.

[33] P.V. Lade, L.B. Ibsen, A study of the phase transformation and the characteristic lines of sand behaviour, in: Proc. Int. Symp. on Deformation and Progressive Failure in Geomechanics, Nagoya, 1997, pp. 353-359.

[34] Y. Vaid, S. Sivathayalan, Fundamental factors affecting liquefaction susceptibility of sands, Canadian Geotechnical Journal, 37(3) (2000) 592-606.

[35] M. Yoshimine, P. Robertson, C. Wride, Undrained shear strength of clean sands to trigger flow liquefaction, Canadian Geotechnical Journal, 36(5) (1999) 891-906.

[36] M. Yoshimine, K. Ishihara, Flow potential of sand during liquefaction, Soils and foundations, 38(3) (1998) 189-198.

[37] S. Shibuya, D. Hight, R. Jardine, Local boundary surfaces of a loose sand dependent on consolidation path, Soils and Foundations, 43(3) (2003) 85-93.

HOW TO CITE THIS ARTICLE

A. Mohammadi, H. Bahadori, Investigating the Effect of Particle Size on the Anisotropic Behavior of Saturated Sands, Using Hollow Cylindrical Torsional Shear Apparatus, AUT J. Civil Eng., 4(4) (2020) 449-472

DOI: 10.22060/ajce.2020.16390.5584